Table 2 (*continued*)

Gene symbol	*Acc. no.*	*Gene name*	*No. of appearance of the genes*		
			HBL with positive AFP	*Normal infant's liver*	*HBL with negative AFP*
CYP3A4	M18907	P450	6	81	3
AHSG	M16961	Alpha-2-HS-glycoprotein	6	5	2
TPT1	X16064	Translationally controlled tumor protein	6	0	3
CYP2C9	M61855	P4502C9	1	10	1

other hand, genes involved in protein synthesis such as elongation factors and ribosomal proteins were observed more frequently in HBLs than in normal liver. The expression profile in the library of the tumor without AFP secretion was very different from that with positive AFP (HMFT *vs* HKMT). As expected, *AFP* gene did not appear in the HKMT library. Intriguingly, *Wnt Inhibitory factor-1* and *dickkopf*, both of which are inhibitors of Wnt signaling (Hsieh *et al*., 1999; Wang *et al*., 2000), frequently appeared in the HKMT library. In addition, *vimentin*, *RNA-binding motif protein*, and *RAP1B* also frequently appeared in the HKMT library, but hardly in the HMFT library with AFP secretion. Thus, HBL with positive AFP and that with negative AFP seem to have a distinct gene expression profile, resulting in different biological characteristics.

Identification of the differentially expressed genes between HBLs and normal livers

To identify differentially expressed genes between HBLs and their corresponding normal livers, 1188 independent genes which included all of the 847 genes with unknown function and 341 known genes that were related to cellular functions including cell growth and differentiation among the 10431 cDNAs were selected and subjected to semiquantitative RT–PCR analysis (Figure 1a). The complementary DNAs reverse-transcribed from total RNA obtained from eight tumors and their corresponding normal livers were used as PCR templates after normalization with *GAPDH* expression. As a result, we found that 75 genes were expressed at higher levels in normal livers than in HBLs, whereas only 11 genes were expressed at higher levels in the tumors than in normal livers. Figure 1a shows the representatives of the results of differential screening using semi-quantitative RT–PCR and Table 3 lists 46 differentially expressed genes with known functions. We classified those differentially expressed genes into 12 categories according to their known functions. The genes preferentially expressed in normal liver showed the profiles which reflected normal liver function. Consistent with the previous reports about HBL and hepatocellular carcinoma (von Horn *et al*., 2001; Xu *et al*., 2001; Kinoshita and Miyata, 2002), *Insulin-like growth factor binding protein-3* (*IGFBP-3*), *aldolase B*, *ceruloplasmin*, and *c-reactive protein* were downregulated in HBLs as compared with the normal livers. The expression of *IGF2*, whose product has mitogenic

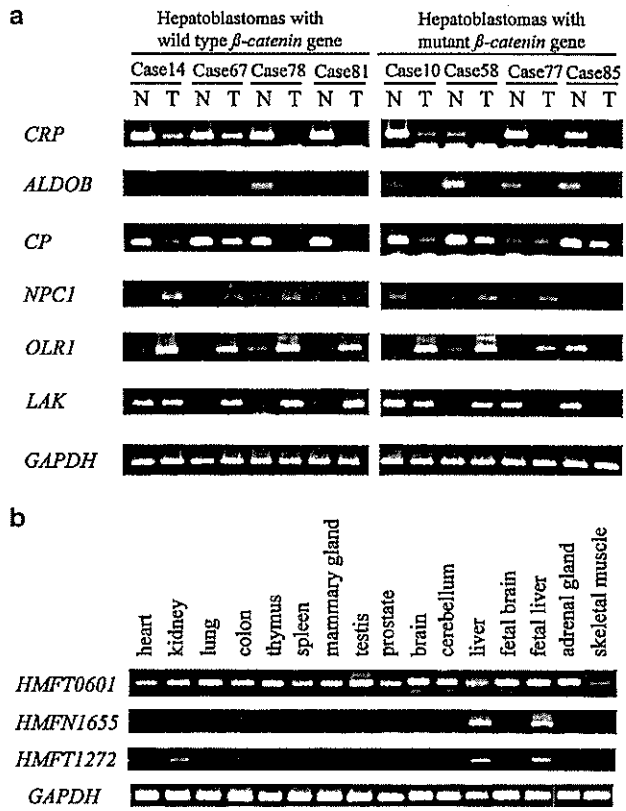

Figure 1 Expression of the representative genes by semi-quantitative RT–PCR. (**a**) Differentially expressed genes between HBLs with or without *β-catenin* mutation and the corresponding normal livers. cDNA was synthesized from RNAs prepared from eight pairs of tumors and their corresponding normal livers, and was used as a PCR template. Amount of cDNAs was normalized to that of *GAPDH*. Four tumors (cases 14, 67, 78, and 81) were with wild-type *β-catenin* gene, while the other four tumors (cases 10, 58, 77, and 85) were with mutant *β-catenin* gene. Gene symbols were shown on the left; *CRP*: C-reactive protein, *ALDOB*: aldolase, *CP*: ceruloplasmin, *NPC1*: Niemann–Pick disease, type C1, *OLR1*: oxidized low-density lipoprotein receptor 1, *LAK*: lymphocyte alpha-kinase. N: normal, T: tumor. (**b**) Semiquantitative RT–PCR of multiple human tissues. *HMFT0601* exhibited ubiquitous expression in all tissues examined, whereas *HMFN1655* and *HMFT1272* showed specific expression in liver and fetal liver

activity, is upregulated in HBLs, suggesting that the IGF axis may be involved in development of the tumor (Gray *et al*., 2000).

Four known genes which were expressed at high levels in HBLs (tumor > normal liver) include GTP-binding

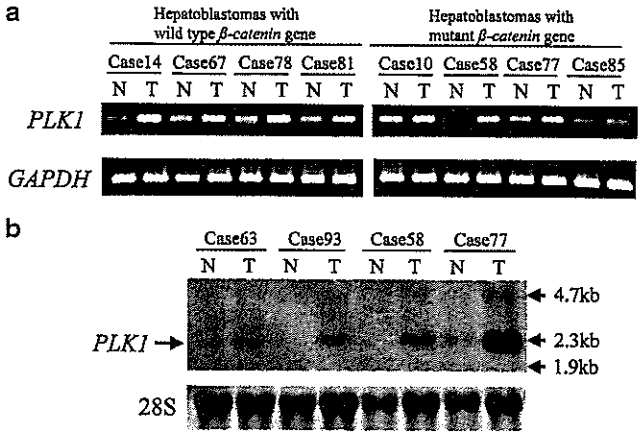

Figure 2 Increased expression of *PLK1* in HBLs. (a) Semiquantitative RT–PCR of *PLK1* gene in eight HBL cases. Preferential expression of the *PLK1* was seen in all sample pairs with and without *β-catenin* mutation. (b) Northern blot analysis of *PLK1* in primary HBLs, The 28S ribosomal band is shown as a control of each RNA amount

nuclear protein gene *RAN*, *PLK1* onocgene, and two cholesterol metabolism-associated protein genes, *low-density lipoprotein (LDL) receptor 1* and *Niemann-Pick disease type C1 (NPC1)*. The RAN protein is involved in the control of nucleo-cytoplasmic traffic of many nuclear proteins through formation of the transport nuclear pore complex (Ribbeck *et al.*, 1998). Nagata *et al.* (2003) also reported that *RAN* is upregulated in HBLs by oligonucleotide DNA array experiment. The LDL receptor 1 binds LDL, a major plasma cholesterol-carrying lipoprotein, and plays an important role in cholesterol homeostasis (Sudhof *et al.*, 1987; Goldstein and Brown, 1990; Hamanaka *et al.*, 1992). *NPC1* is a causal gene of Niemann–Pick type C disease which is an autosomal recessive lipid storage disorder that affects the viscera and central nervous system (Brady *et al.*, 1989). It encodes a protein with sequence similarity to the morphogen receptor 'patched', and to the cholesterol-sensing regions of 3-hydroxy-3-methylglutaryl coenzyme A (HMG-CoA) reductase (Loftus *et al.*, 1997) and is involved in the intracellular trafficking of cholesterol. Concerning the differentially expressed genes which contained unknown sequences, those cDNA sequences have been submitted to the public database (Genbank/DDBJ Accession numbers: AB07 3346-AB073347, AB073382-AB073387, AB073599-AB0 73614, and AB075869-AB075881). Interestingly, only one known gene, *lymphocyte alpha-kinase (LAK)*, showed distinct expression pattern between HBLs with mutant *β-catenin* and those with wild type *β-catenin* (Figure 1a).

We next examined expression pattern of the novel genes in human multiple tissues by semi-quantitative RT–PCR and found that at least five genes were specifically expressed in the liver (a part of the data is shown in Figure 1b). Since the oncogene *PLK1* (*polo-like kinase-1*) was expressed in HBLs at significantly high levels as compared with the corresponding normal livers, we further examined the role of its expression in HBL.

PLK1 oncogene is overexpressed in HBLs

Recent studies have demonstrated that the preferential expression of *PLK1* mRNA is associated with some cancers including non-small-cell lung cancer (Wolf *et al.*, 1997), squamous cell carcinoma of the head and neck (Knecht *et al.*, 1999), and esophageal carcinoma (Tokumitsu *et al.*, 1999). However, the role of *PLK1* in HBL has never been reported. As indicated by semi-quantitative RT–PCR described above, we found that *PLK1* mRNA expression in HBLs is higher than in normal livers (Figure 2a). Northern blot analysis also confirmed its higher expression in HBLs (Figure 2b). We also performed Southern blot analysis by using the genomic DNAs obtained from primary HBLs and human placenta as a control, and probed with the *PLK1*-specific DNA fragment. However, we failed to find any clue of rearrangements or amplification of the *PLK1* gene locus (data not shown).

To examine the clinical significance of the expression level of *PLK1*, we performed quantitative real-time RT–PCR analysis using 74 primary hepatoblastomas and 29 corresponding normal liver samples (Figure 3a). The average arbitrary values of *PLK1* expression in HBLs and normal livers were 28.9 ± 6.7 and 4.1 ± 0.76, respectively (mean $\pm$ s.e.m., $P < 0.01$). The average values in alive and dead cases were 21.7 ± 5.2 ($n = 61$) and 62.4 ± 28.2 ($n = 13$), respectively ($p = 0.021$). When we compared the expression levels of *PLK1* between 24-paired HBLs and their corresponding normal livers, the former in HBL samples was significantly higher in comparison with the latter ($P < 0.01$) (Figure 3b). We also examined the relationship between the expression levels of *PLK1* and clinicopathological data of HBLs. Statistically significant correlation was observed only between histology and *PLK1* expression ($p = 0.041$). The expression level of *PLK1* in the tumors with poorly differentiated histology was higher than those with the well-differentiated one. The other clinicopathological factors such as age, clinical stage, and *β-catenin* mutation did not show a statistical significance with *PLK1* expression.

To further examine whether the *PLK1* expression was associated with the outcome of the patients with HBL, we performed a Kaplan–Meier analysis (Figure 4). The distinction between high and low levels of *PLK1* expression was based on the median value (low, *PLK1* < 13 d.u.; high, *PLK1* $\geq$ 13 d.u.). Since the overall survivals of 15 out of 74 cases were unknown, 59 cases were applied to the analysis. The 5-year survival rates of the groups with high and low *PLK1* expression were 55.9 and 87.0%, respectively ($P = 0.042$). The univariate analysis showed that both *PLK1* expression ($P = 0.015$) and histology ($P = 0.025$) have a significant prognostic importance (Table 4). The multivariate analysis demonstrated that *PLK1* expression was significantly related to survival, after controlling *β-catenin* mutation, age, stage,

Table 3 The known genes differentially expressed between hepatoblastomas and normal livers

	Gene symbol	*Acc. no*	*Gene name*
Protein synthesis, metabolism, transport			
T>N	RAN	NM_006325	GTP-binding nuclear protein RAN
N>T	LBP	AF105067	Lipopolysaccharide-binding protein
N>T	TDO2	BC005355	Tryptophan 2,3-dioxygenase
N>T	CRP	X56692	C-reactive protein
N>T	GC	NM_000583	Group-specific component
N>T	HP	K01763	Haptoglobin
N>T	HPX	NM_000613	Hemopexin
N>T	SQSTM1	NM_003900	Sequestosome 1
N>T	PHDGH	AF171237	A2-53-73 3-phosphoglycerate dehydrogenase
N>T	PPP1R3C	XM_005398	Protein phosphatase 1, regulatory (inhibitor) subunit 3C
N>T	ITIH4	D38595	Inter-alpha-trypsin inhibitor family heavy chain-related protein
N>T	G1P2	M13755	Interferon-induced 17-kDa/15-kDa protein
Cytokine, growth factor, hormones			
N>T	HABP2	D49742	Hyaluronan binding protein 2
N>T	IGFBP3	NM_000598	Insulin-like growth factor binding protein 3
N>T	GOT1	AF052153	Glutamic-oxaloacetic transaminase 1
Cell signaling			
N>T	CSNK2B	M30448	Casein kinase II, beta polypeptide
N>T	TPD52	NM_005079	Tumor protein D52
cell cycle			
T>N	PLK1	X73458	PLK1
Cell structure, adhesion			
N>T	LRG	AF403428	Leucine-rich alpha-2-glycoprotein
N>T	PGRP-L	AF384856	Peptidoglycan recognition protein L precursor
N>T	CLDN4	NM_001305	Claudin4
N>T	VTN	NM_000638	Vitronection
Organism defense			
N>T	RODH-4	NM_003708	Retinol dehydrogenase 4
N>T	MASP1	AF284421	Mannan-binding lectin serine protease 1
N>T	C4BPA	M31452	Complement component 4 binding protein, alpha
Glycometabolism			
N>T	ADH1B	AF153821	Alcohol dehydrogenase 1B, beta polypeptide
N>T	ALDOB	M15657	Aldolase B
Lipid metabolism			
T>N	NPC1	NM_000271	Niemann–Pick disease, type C1
T>N	OLR1	NM_002543	Oxidized low density lipoprotein (lectin-like) receptor 1
N>T	DGAT2	AF384161	Diacylglycerol acyltransferase
N>T	SCP2	NM_002979	Sterol carrier protein 2
N>T	APOA5	AF202890	Apolipoprotein A-V
N>T	AADAC	L32179	Arylacetamide deacetylase
N>T	SAA4	M81349	Amyloid A protein
Transcription			
N>T	BZW1	NM_014670	Basic leucine zipper and W2 domains 1
N>T	CREB-H	NM_032607	CREB/ATF family transcription factor
RNA biogenesis, metabolism			
N>T	HNRPDL	AB017018	Heterogeneous nuclear ribonucleoprotein D-like
Homeostasis, heat shock protein, metabolic enzymes			
N>T	UGT1A	AF297093	UGT1 gene locus
N>T	ALPL	X14174	Liver-type alkaline phosphatase
N>T	SLC10A1	L21893	Solute carrier family 10
N>T	CES1	AF177775	Carboxylestelase
N>T	AKR1D1	Z28339	Aldo-keto reductase family 1, member D1
N>T	AKR1C2	U05598	Aldo-keto reductase family 1, member C2
N>T	CP	D45045	Ceruloplasmin
Others			
N>T	DGCR6L	NM_033257	DiGeorge syndrome critical region gene 6 like
N>T	A1BG	AF414429	Alpha-1-B glycoprotein

T>N: highly expressed in the tumors as compared to normal livers. N>T: highly expressed in normal livers as compared to the tumors

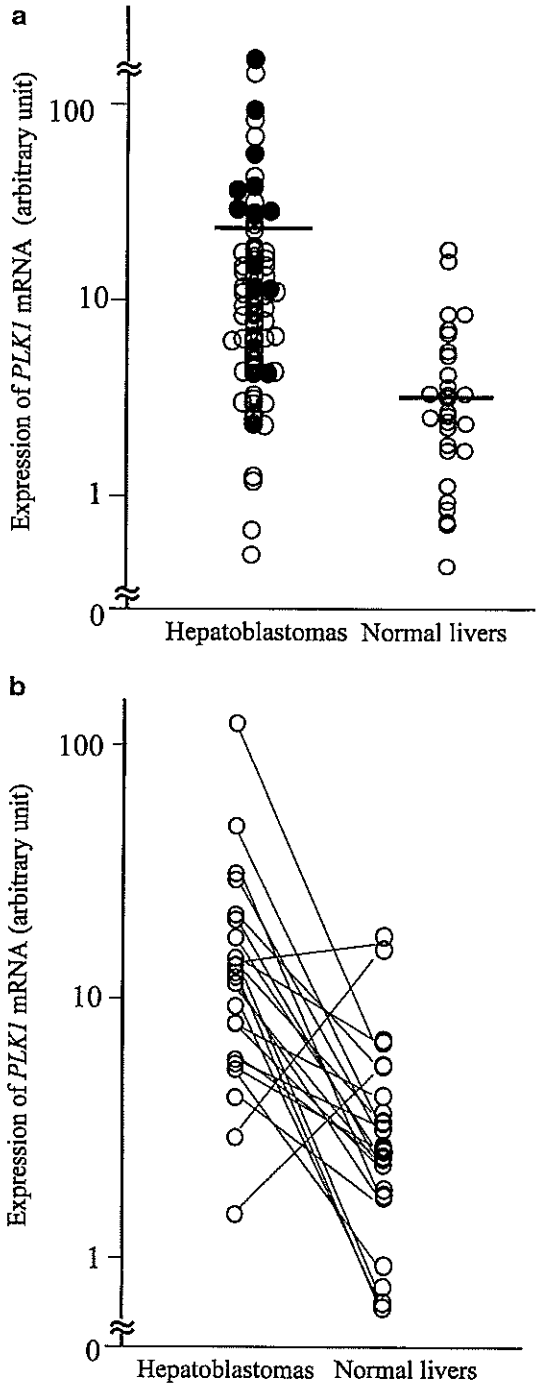

Figure 3 mRNA expression of *PLK1* in HBLs and the corresponding normal livers measured by quantitative real-time RT–PCR. (**a**) The levels of *PLK1* mRNA expression in HBLs and normal livers. The expression levels of *PLK1* were determined by quantitative real-time RT–PCR analysis using 74 HBL tissues and 29 normal livers (see Materials and methods). The *PLK1* expression values were normalized by *GAPDH*. Open and closed circles represent alive and dead, respectively. Since the values of the *PLK1* expression were skewed, a log transformation was used for the expression values. The bars show mean values. (**b**) Correlation of *PLK1* expression between HBL and its corresponding normal liver in 24 paired samples

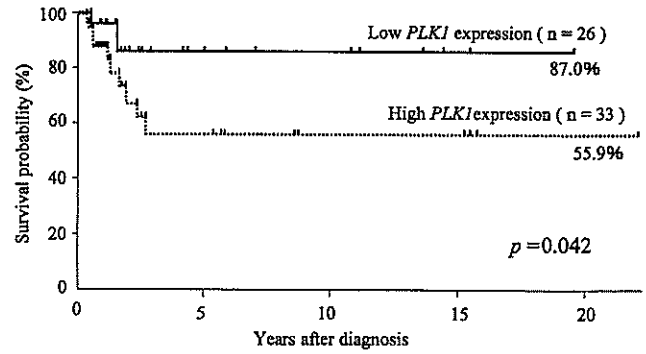

Figure 4 Kaplan–Meier survival curves ($n = 59$) in relation to the expression levels of *PLK1* (median cutoff). The arbitrary median cutoff value was set as 13. The patients with high expression of *PLK1* represented significantly poor prognosis than those with its low expression

Table 4 Univariate Cox regression analysis using *PLK1*(log) and dichotomous factors of *β-catenin* mutation, age, stage, and histology ($n = 59$)

Factor	n	P-*value*	*HR (95% CI)*
PLK1(log)	59	0.015	1.62 (1.10, 2.40)
β-catenin (mutant vs wild type)	58	0.27	1.85 (0.62, .5.56)
Age (>1 vs ≤1 year)	55	0.76	1.22 (0.33, 4.52)
Stage (3, 4 vs 1, 2)	56	0.083	3.81 (0.84, 17.2)
Histology (poorly vs well)	53	0.025	4.48 (1.21, 16.6)

All variables with two categories, except *PLK1*(log); HR = hazard ratio shows the relative of death of first category relative to second; CI = confidence interval

or histology, but marginally related to survival after controlling both histology and stage (Table 5).

Discussion

HBL is one of the embryonal tumors in close relation to the normal as well as abnormal tissue development. To understand the molecular basis of the genesis of HBL, here we randomly cloned a large number of genes expressed in HBLs with or without AFP production and in a non-tumorous infant's liver. Extensive screening for the differentially expressed genes between the tumors and their corresponding normal livers has successfully identified at least 86 genes including 40 with unknown function, which may potentially contribute to develop new therapeutic strategies against HBLs with poor prognosis.

HBL cDNA libraries

We have identified the genes with unknown function in approximately 8% of the total 10431 clones obtained from our oligo-capping cDNA libraries. The comparison of the frequently appeared genes in each libraries shows that expression profile is relatively similar between AFP-positive HBL and the normal part of the infant's liver, whereas it is very different between AFP-positive and AFP-negative tumors, in which many genes

Table 5 Multivariable Cox regression analysis using *PLK1*(log) and dichotomous factors of *β-catenin* mutation, age, stage, and histology ($n = 50$)

Variable	P-*value*	*Variable*	P-*value*	*Variable*	P-*value*
PLK1(log)	0.009	*β-catenin* (mutant vs. wild type)	0.51		
PLK1(log)	0.005	Age (>1 vs ≤1 year)	0.92		
PLK1(log)	0.019	Stage (3, 4 vs 1, 2)	0.46		
PLK1(log)	0.027	Histology (poorly vs well)	0.12		
PLK1(log)	0.052	Histology (poorly vs well)	0.12	Stage (3, 4 vs 1, 2)	0.47

All variables with two categories, except *PLK1*(log)

are downregulated (Table 2). In the library of the latter tumor, *vimentin*, *RNA-binding motif protein*, *Wnt inhibitory factor-1*, *dickkopf*, and *RAP1B* are frequently appeared, whereas they are hardly appeared in the other libraries. Wissmann *et al.* (2003) have recently reported that *WIF1* is downregulated in various cancers (prostate cancer, breast cancer, non-small-cell lung cancer, and bladder cancer), and suggested that loss of WIF1 expression may be an early event in tumorigenesis in those tissues. It is notable that, in contrast to AFP-positive HBLs, the patient's outcome of the tumor with negative AFP is very poor, though the incidence of the latter tumor is low (von Schweinitz *et al.*, 1995). This suggests that AFP-positive and AFP-negative HBLs have a different genetic as well as biological background. In addition, recent reports have demonstrated that frequent mutation of the *β-catenin* gene and nuclear accumulation of its protein product are one of the main causes of the tumorigenesis of HBL. The *APC* and *Axin* genes are also mutated in some HBLs (Oda *et al.*, 1996; Miao *et al.*, 2003; Thomas *et al.*, 2003), indicating that Wnt signaling pathway plays an important role in causing the tumors, most of which are AFP-positive. Therefore, the poor-prognostic HBL without producing AFP might be caused by the particular mechanism additional to or other than the abnormality of Wnt signaling pathway. Although the appearance frequency of the genes in each library does not always reflect the actual expression levels of each gene, it may at least in part show the differences among the tumor subsets with different genetic abnormalities. As our libraries contain many genes involved in liver development, normal liver functions, and carcinogenesis, they must be useful for making a liver-proper cDNA microarray to analyse expression profiles of HBL, viral infection-induced hepatitis, liver cirrhosis, and HCC.

Differentially expressed genes between HBLs and the corresponding normal livers

cDNA microarray, which is often applied to a comprehensive gene expression analysis, is able to detect many genes that are differentially expressed between tumors and normal tissues (Okabe *et al.*, 2001; Nagata *et al.*, 2003). However, it is expensive and needs further confirmation of the selected genes by a semi-quantitative RT–PCR or a real-time RT–PCR method. Therefore, using semi-quantitative RT–PCR and the specific primers of 1188 cDNAs, we have identified 86 genes differentially expressed between HBLs and their corresponding normal livers. Surprisingly, 75 out of 86 genes are preferentially expressed in the latter tissues, and only 11 including *RAN*, *PLK1*, *NPC1*, and *OLR1* known genes are expressed at high levels in HBLs. One of the reasons of this result may be that many gene products, which are necessary for full function in the matured liver metabolism, are dispensable for the malignant growth of the tumor except for the very limited genes. The results of some differentially expressed genes are consistent with those in the previous reports. von Horn *et al.* (2001) have shown that the mRNA levels of *insulin-like growth factor-binding proteins* including *IGFBP-3* are decreased in HBLs than in normal livers. Kinoshita and Miyata (2002) have also reported that *aldolase B* mRNA is downregulated in over 50% of 20 HCCs examined. They proposed that the measurement of aldolase activity in serum is useful to determine the number of collapsed hepatic cells in cirrhosis. Recently, evidences suggest that not only mutant β-catenin but also wild-type β-catenin localize in the cellular nuclei of HBL as well as some other cancers (Rimm *et al.*, 1999; Takayasu *et al.*, 2001). The increased expression of the *Ran* gene in HBLs might be correlated with the shuttling of β-catenin and/or other related proteins between cytoplasm and nucleus in the tumor cells.

Owing to constitutive activation of Wnt signaling in most of the HBLs, the 86 genes differentially expressed between the tumor and its corresponding normal liver were expected to contain downstream target genes of Wnt signaling pathway that might regulate early stage of the hepatic development. In this study, however, only the *lymphocyte alpha-kinase* (*LAK*) gene was found to be differentially expressed at high levels in HBLs with wild-type *β-catenin* and at low levels in those with *β-catenin* mutation. LAK is a new class of protein kinases with a novel catalytic domain, but its precise function is currently unknown (Ryazanov *et al.*, 1999). Thus, our result may suggest that the target genes of the Wnt signaling pathway are commonly affected in HBLs, regardless of the presence or absence of *β-catenin* mutation.

PLK1 as a prognostic indicator of HBL

PLK1 (*polo-like kinase 1*), the human counterpart of *polo* in *Drosophila melanogaster* and of *CDC5* in *Saccharomyces cerevisiae*, encodes a serine/threonine kinase with polo-box domains (Clay *et al.*, 1993). PLK1 is crucial for various events of mitotic progression including centrosome maturation (Lane and Nigg,

1996), spindle function (Glover *et al.*, 1996), activation of cyclin B/Cdc2 (Qian *et al.*, 1998; Toyoshima-Morimoto *et al.*, 2001), and regulation of anaphase-promoting complex (Kotani *et al.*, 1998; Nigg, 1998). Elevated expression of *PLK1* is also found in different types of adult cancers including non-small-cell lung cancer, head and neck tumors, esophageal carcinomas, melanomas, and colorectal cancers (Wolf *et al.*, 1997; Knecht *et al.*, 1999; Tokumitsu *et al.*, 1999; Dietzmann *et al.*, 2001; Takai *et al.*, 2001), implying its critical role in tumorigenesis. In the present study, we have found that *PLK1* is upregulated in primary HBLs, and that its mRNA expression levels are significantly correlated with poor outcome of the patients. Multivariate Cox regression analysis indicated that *PLK1* expression could be an independent prognostic factor from *β-catenin* mutation, age, stage, or histology. However, clinical stage did not show a significant correlation with *PLK1* expression, though it is one of the critical prognostic markers. One of the possible reasons may be that the 59 tumors we used for statistical analysis include two unusual patients, one had stage 4 tumor with good prognosis and another case had stage 1 tumor with poor prognosis. These might have reduced the significance of the tumor stage in patients' survival in our sample set.

It is notable that, among the 1188 genes we have screened for differential expression, *PLK1* is the only one known oncogene overexpressed in the HBL tissues. Smith *et al.* (1997) have reported that constitutive expression of *PLK1* in NIH3T3 cells causes oncogenic focus formation and forms tumors in nude mice. Furthermore, Liu and Erikson (2003) have recently shown that the application of small interfering RNA which specifically depletes *PLK1* expression in cancer cells inhibits cell proliferation, arrests cell cycle, and induces apoptosis. Thus, PLK1 may play a crucial role in causing HBL and other cancers. It may be interesting to examine whether *PLK1* is a target of β-catenin transported from the cytosol into the nucleus. The disruption of PLK1 function could be a future therapeutic tool for the aggressive type of hepatoblastomas.

In conclusion, our HBL cDNA project has provided a large number of genes related to liver development, metabolism, and carcinogenesis. We are currently applying these genes to the cDNA microarray system. Our cDNA resource should be an important tool to understand the molecular mechanism of the genesis of HBL as well as to develop new diagnostic and therapeutic strategies against the aggressive tumors in the future.

Materials and methods

Clinical materials

Tumor tissues and their corresponding normal liver tissues were frozen at the time of surgery and stored at −80°C until use. All specimens were provided from the Tissue Bank of the Japanese Study Group for Pediatric Liver Tumor (JPLT) (Uotani *et al.*, 1998). A total of 74 HBL samples (seven were classified as being stage 1, 17 as stage 2, 26 as stage 3, 15 as stage 4, and nine were unknown stages) were used in this study. The tumors were staged according to the Japanese histopathological classification of HBL (Hata, 1990). From 1991 to 1999, HBLs had been treated by combination chemotherapy using cisplatin and THP-adriamycin according to the JPLT-1 protocol (Sasaki *et al.*, 2002). After 2000, a more intensive chemotherapeutic regimen, ITEC (ifosfamide, THP-adriamycin, etoposide, and carboplatin), has been utilized for tumors that prove resistant to the combination chemotherapy in the JPLT-2 study. Among the 74 tumor samples we examined, 36 and 35 tumor tissues were obtained prior to and after chemotherapy, respectively, and the remaining three were unknown. In the same sample set, 59 tumors were accompanied by outcome information and used for making survival curves, among which 31 and 28 tissues were obtained prior to and after chemotherapy, respectively. Tumor histology was also classified according to Hata (1990). 'Poor histology' indicates 'poorly differentiated (embryonal type)', and 'well histology' indicates 'well-differentiated (fetal type)'. The informed consents were obtained in each institution or hospital. High molecular weight DNA and total RNA of these samples were prepared as described previously (Ichimiya *et al.*, 1999).

Construction of oligo-capping cDNA libraries

Four oligo-capping cDNA libraries, two (HMFT, HYST) derived from HBLs with secretion of AFP, one (HKMT) from HBL without AFP secretion, and one (HMFN) from the corresponding normal liver, were constructed according to the method previously described (Suzuki *et al.*, 1997). These were approved by the institutional review board. The oligo-capping method enables full-length cDNA cloning with high efficiency. The 12 000 cDNA clones in total were randomly picked up and single-run sequencing was performed. Nucleotide sequence of both ends for each cDNA clone was homology-searched against the public nucleotide database using the BLAST program at the National Center for Biotechnology Information (NCBI) (Genbank release 122, January 2001).

Differential screening of the genes by semi-quantitative RT–PCR

The eight samples were selected as PCR templates to screen for the differentially expressed genes. Cases 58 and 81 were defined as stage 2 HBL, cases 10, 67, 78, and 85 were in stage 3, case 14 was in stage 4. Among those eight tumors, four (cases 14, 67, 78, and 81) had the mutant *β-catenin*, and the others (cases 10, 58, 77, and 85) not. Mutation analysis for *β-catenin* was performed as described previously (Takayasu *et al.*, 2001). The differential expression of the genes between the HBL and normal livers was confirmed at least twice using semi-quantitative RT–PCR. The individual gene-specific PCR primer sequences were determined by using Primer3 program (provided at Washington University). For cDNA templates, 5 μg of total RNA was converted to cDNA using random primers (Takara, Otsu, Japan) with SuperScript II RNaseH$^-$ reverse transcriptase (Gibco BRL, Rockville, MD, USA). Those cDNAs were at first amplified with *GAPDH* primers for 27 cycles and the amounts of the PCR products were measured by ALF Express™ sequencer and normalized. The amplification was performed 35 or 40 cycles of 95°C for 30 s, 57 or 59 or 61°C for 15 s and 72°C for 60 s, and the final extension was at 72°C for 5 min, using a Perkin-Elmer Thermalcycler 9700 (Perkin-Elmer, Foster City, CA, USA). The PCR products

were run on 2% agarose gels and stained with ethidium bromide. We defined the gene as differentially expressed when it exhibits differential expression between the tumor and its corresponding normal liver in more than four out of the eight samples.

Northern blot analysis

In all, 25 μg of total RNA from the primary HBLs, HCC, and their corresponding normal livers were subjected to Northern analysis. Total RNA was prepared according to the method of Chomczynski and Sacchi (1987). Total RNA was fractionated by electrophoresis on 1% agarose gel containing formaldehyde, transferred onto a nylon membrane filter, and immobilized by UV crosslinking. The hybridization cDNA probe was a 976-base pair human *PLK1* cDNA fragment and labeled with [α-^{32}P]-dCTP using the BcaBEST random priming kit (Takara Biomedicals). The filter was hybridized at 65°C in a solution containing 1 M NaCl, 1% SDS, 7.5% dextran sulfate, 100 μg/ml of heat-denatured salmon sperm DNA, and radiolabeled probe DNA.

Quantitative real-time RT–PCR of PLK1

The primer set for amplification of the *PLK1* and probe sequence are as follows: forward primer, 5′-GCTGCACAAG AGGAGGAAA-3′; reverse primer, 5′-AGCTTGAGGTCTC-GATGAATAAC-3′; probe, 5′-CCTGACTGAGCCTGAGG CCCGATAC-TA-3′. Taqman *GAPDH* control reagents (Perkin-Elmer/Applied Biosystems) were used for the amplification of *GAPDH* as recommended by the manufacturer. PCR was performed using ABI Prism 7700 Sequence Detection System (Perkin-Elmer/Applied Biosystems). In all, 2 μl of cDNA was amplified in a final volume of 25 μl containing 1 × Taqman PCR reaction buffer, 200 μM each dNTP, 0.9 μM each primer, and 200 nM Taqman probe. The optional thermal cycling condition was as follows: 40 cycles of a two-step PCR (95°C for 15 s, 60°C for 60 s) after the initial denaturation (95°C for 10 min). Experiments were carried out in triplicate for each data point.

Statistical analysis

Statistical analyses were performed using Mann–Whitney's *U*-test and Cox regression. A *P*-value of less than 0.05 was considered significant.

Acknowledgements
We are grateful to Shigeru Sakiyama and Toshinori Ozaki for critical reading of the manuscript, and Yoko Nakamura and Aiko Morohashi for experimental support. We thank Eriko Isogai, Naoko Sugimitsu, and Yuki Nakamura for preparing RNA and sequencing analysis, and Natsue Kitabayashi, Emiko Kojima, Emi Goto, and Hisae Murakami for technical assistance. We also thank the hospitals and institutions collaborating with the Japanese Study Group for Pediatric Liver Tumor (JPLT) for providing surgical specimens. This work was supported in part by the fund from Hisamitsu Pharmaceutical Company and a grant-in-aid for Scientific Research on Priority Areas (C) 'Medical Genome Science' from the Ministry of Education, Culture, Sports, Science, and Technology of Japan.

References

Albrecht S, Von Schweinitz D, Waha A, Kraus JA, Von Deimling A and Pietsch T. (1994). *Cancer Res.*, **54**, 5041–5044.
Brady RO, Filling-Katz MR, Barton NW and Pentchev PG. (1989). *Neurol. Clin.*, **7**, 75–88.
Buendia MA. (1992). *Adv. Cancer Res.*, **59**, 167–226.
Buendia MA. (2002). *Med. Pediatr. Oncol.*, **39**, 530–535.
Chomczynski P and Sacchi N. (1987). *Anal. Biochem.*, **162**, 156–159.
Clay FJ, McEwen SJ, Bertoncello I, Wilks AF and Dunn AR. (1993). *Proc. Natl. Acad. Sci. USA*, **90**, 4882–4886.
Dietzmann K, Kirches E, Von Bossanyi, Jachau K and Mawrin C. (2001). *J. Neurooncol.*, **53**, 1–11.
Exelby PR, Filler RM and Grosfeld JL. (1975). *J. Pediatr. Surg.*, **10**, 329–337.
Fukuzawa R, Umezawa A, Ochi K, Urano F, Ikeda H and Hata J. (1999). *Int. J. Cancer*, **82**, 490–497.
Giardiello FM, Petersen GM, Brensinger JD, Luce MC, Cayouette MC, Bacon J, Booker SV and Hamilton SR. (1996). *Gut*, **39**, 867–869.
Glover DM, Ohkura H and Tavares A. (1996). *J. Cell Biol.*, **135**, 1681–1684.
Goldstein JL and Brown MS. (1990). *Nature*, **343**, 425–430.
Gray SG, Eriksson T, Ekstrom C, Holm S, Von Schweinitz D, Kogner P, Sandstedt B, Pietsch T and Ekstrom TJ. (2000). *Br. J. Cancer*, **82**, 1561–1567.
Haas JE, Muczynski KA, Krailo M, Ablin A, Land V, Vietti TJ and Hammond GD. (1989). *Cancer*, **64**, 1082–1095.
Hamanaka R, Kohno K, Seguchi T, Okamura K, Morimoto A, Ono M, Ogata J and Kuwano M. (1992). *J. Biol. Chem.*, **267**, 13160–13165.
Hata Y. (1990). *Jpn. J. Surg.*, **20**, 498–502.
Hata Y, Ishizu H, Ohmori K, Hamada H, Sasaki F, Uchino J, Inoue K, Naitoh H, Fujita M, Kobayashi T and Yokoyama S. (1991). *Cancer*, **68**, 2566–2570.
Hsieh JC, Kodjabachian L, Rebbert ML, Rattner A, Smallwood PM, Samos CH, Nusse R, Dawid IB and Nathans J. (1999). *Nature*, **398**, 431–436.
Ichimiya S, Nimura Y, Kageyama H, Takada N, Sunahara M, Shishikura T, Nakamura Y, Sakiyama S, Seki N, Ohira M, Kaneko Y, McKeon F, Caput D and Nakagawara A. (1999). *Oncogene*, **18**, 1061–1066.
Idilman R, De Maria N, Colantoni A and Van Thiel DH. (1998). *J. Viral. Hepat.*, **5**, 285–299.
Kinoshita M and Miyata M. (2002). *Hepatology*, **36**, 433–438.
Kinzler KW and Vogelstein B. (1996). *Cell*, **87**, 159–170.
Knecht R, Elez R, Oechler M, Solbach C, Von Ilberg C and Strebhardt K. (1999). *Cancer Res.*, **59**, 2794–2797.
Koch A, Denkhaus D, Albrecht S, Leuschner I, Von Schweinitz D and Pietsch T. (1999). *Cancer Res.*, **59**, 269–273.
Kotani S, Tugendreich S, Fujii M, Jorgensen PM, Watanabe N, Hoog C, Hieter P and Todokoro K. (1998). *Mol. Cell*, **1**, 371–380.
Lane HA and Nigg EA. (1996). *J. Cell Biol.*, **135**, 1701–1713.
Li FP, Wendy AT, Seddon J and Holmes GE. (1987). *J. Am. Med. Assoc.*, **257**, 2475–2477.
Li X, Adam G, Cui H, Sandstedt B, Ohlsson R and Ekstrom TJ. (1995). *Oncogene*, **11**, 221–229.
Liu X and Erikson RL. (2003). *Proc. Natl. Acad. Sci. USA*, **100**, 5789–5794.

Loftus SK, Morris JA, Carstea ED, Gu JZ, Cummings C, Brown A, Ellison J, Ohno K, Rosenfeld A, Tagle DA, Pentchev PG and Pavan WJ. (1997). *Science*, **277**, 232–235.
Mann JR, Lakin GE, Leonard JC, Rawlinson HA, Richardson SG, Corkery JJ, Cameron AH and Shah KJ. (1978). *Arch. Dis. Child*, **53**, 366–374.
Miao J, Kusafuka T, Udatsu Y and Okada A. (2003). *Hepatol. Res.*, **25**, 174–179.
Montagna M, Menin C, Chieco-Bianchi L and D'Andrea E. (1994). *J. Cancer Res. Clin. Oncol.*, **120**, 732–736.
Morin PJ, Sparks AB, Korinek V, Barker N, Clevers H, Vogelstein B and Kinzler KW. (1997). *Science*, **275**, 1787–1790.
Nagata T, Takahashi Y, Ishii Y, Asai S, Nishida Y, Murata A, Koshinaga T, Fukuzawa M, Hamazaki M, Asami K, Ito E, Ikeda H, Takamatsu H, Koike K, Kikuta A, Kuroiwa M, Watanabe A, Kosaka Y, Fujita H, Miyake M and Mugishima H. (2003). *Cancer Genet. Cytogenet.*, **145**, 152–160.
Nigg EA. (1998). *Curr. Opin. Cell Biol.*, **10**, 776–783.
Oda H, Nakatsuru Y, Imai Y, Sugimura H and Ishikawa T. (1995). *Int. J. Cancer*, **60**, 786–790.
Oda H, Imai Y, Nakatsuru Y, Hata J and Ishikawa T. (1996). *Cancer Res.*, **56**, 3320–3323.
Okabe H, Satoh S, Kato T, Kitahara O, Yanagawa R, Yamaoka Y, Tsunoda T, Furukawa Y and Nakamura Y. (2001). *Cancer Res.*, **61**, 2129–2137.
Okubo K, Hori N, Matoba R, Niiyama T, Fukushima A, Kojima Y and Matsubara K. (1992). *Nat. Genet.*, **2**, 173–179.
Ortega JA, Krailo MD, Haas JE, King DR, Ablin AR, Quinn JJ, Feusner J, Campbell JR, Lloyd DA, Cherlow J and Hammond GD. (1991). *J. Clin. Oncol.*, **9**, 2167–2176.
Park WS, Oh RR, Park JY, Kim PJ, Shin MS, Lee JH, Kim HS, Lee SH, Kim SY, Park YG, An WG, Kim HS, Jang JJ, Yoo NJ and Lee JY. (2001). *J. Pathol.*, **193**, 483–490.
Polakis P. (1999). *Curr. Opin. Genet. Dev.*, **9**, 15–21.
Qian YW, Erikson E, Li C and Maller JL. (1998). *Mol. Cell. Biol.*, **18**, 4262–4271.
Rainier S, Dobry CJ and Feinberg AP. (1995). *Cancer Res.*, **55**, 1836–1838.
Ribbeck K, Lipowsky G, Kent HM, Stewart M and Gorlich D. (1998). *EMBO J.*, **17**, 6587–6598.
Rimm DL, Caca K, Hu G, Harrison FB and Fearon ER. (1999). *Am. J. Pathol.*, **154**, 325–329.
Ryazanov AG, Pavur KS and Dorovkov MV. (1999). *Curr. Biol.*, **9**, R43–45.
Sasaki F, Matsunaga T, Iwafuchi M, Hayashi Y, Ohkawa H, Ohira M, Okamatsu T, Sugito T, Tsuchida Y, Toyosaka A, Nagahara N, Nishihira H, Hata Y, Uchino J, Misugi K and Ohnuma N. (2002). *J Pediatr Surg.*, **37**, 851–856.
Smith MR, Wilson ML, Hamanaka R, Chase D, Kung H, Longo DL and Ferris DK. (1997). *Biochem. Biophys. Res. Commun.*, **234**, 397–405.
Sudhof TC, Russell DW, Brown MS and Goldstein JL. (1987). *Cell*, **48**, 1061–1069.
Suzuki Y, Yoshitomo-Nakagawa K, Maruyama K, Suyama A and Sugano S. (1997). *Gene*, **200**, 149–156.
Takai N, Miyazaki T, Fujisawa K, Nasu K, Hamanaka R and Miyakawa I. (2001). *Cancer Lett.*, **164**, 41–49.
Takayasu H, Horie H, Hiyama E, Matsunaga T, Hayashi Y, Watanabe Y, Suita S, Kaneko M, Sasaki F, Hashizume K, Ozaki T, Furuuchi K, Tada M, Ohnuma N and Nakagawara A. (2001). *Clin. Cancer Res.*, **7**, 901–908.
Taniguchi K, Roberts LR, Aderca IN, Dong X, Qian C, Murphy LM, Nagorney DM, Burgart LJ, Roche PC, Smith DI, Ross JA and Liu W. (2002). *Oncogene*, **21**, 4863–4871.
Thomas D, Pritchard J, Davidson R, McKiernan P, Grundy RG and de Ville de Goyet J. (2003). *Eur. J. Cancer*, **39**, 2200–2204.
Tokumitsu Y, Mori M, Tanaka S, Akazawa K, Nakano S and Niho Y. (1999). *Int. J. Oncol.*, **15**, 687–692.
Toyoshima-Morimoto F, Taniguchi E, Shinya N, Iwamatsu A and Nishida E. (2001). *Nature*, **410**, 215–220.
Uotani H, Yamashita Y, Masuko Y, Shimoda M, Murakami A, Sakamoto T, Tazawa K and Tsukada K. (1998). *J. Pediatr. Surg.*, **33**, 639–641.
Van Tornout JM, Buckley JD, Quinn JJ, Feusner JH, Krailo MD, King DR, Hammond GD and Ortega JA. (1997). *J. Clin. Oncol.*, **15**, 1190–1197.
Velculescu VE, Vogelstein B and Kinzler KW. (2000). *Trends Genet.*, **16**, 423–425.
Von Horn H, Tally M, Hall K, Eriksson T, Ekstrom TJ and Gray SG. (2001). *Cancer Lett.*, **162**, 253–260.
Von Schweinitz D, Hecker H, Harms D, Bode U, Weinel P, Burger D, Erttmann R and Mildenberger H. (1995). *J. Pediatr. Surg.*, **30**, 845–852.
Von Schweinitz D, Wischmeyer P, Leuschner I, Schmidt D, Wittekind C, Harms D and Mildenberger H. (1994). *Eur. J. Cancer*, **30A**, 1052–1058.
Wang J, Shou J and Chen X. (2000). *Oncogene*, **19**, 1843–1848.
Weber RG, Pietsch T, Von Schweinitz D and Lichter P. (2000). *Am. J. Pathol.*, **157**, 571–578.
Wei Y, Fabre M, Branchereau S, Gauthier F, Perilongo G and Buendia MA. (2000). *Oncogene*, **19**, 498–504.
Weinberg AG and Finegold M. (1983). *Hum. Pathol.*, **14**, 512–537.
Wissmann C, Wild PJ, Kaiser S, Roepcke S, Stoehr R, Woenckhaus M, Kristiansen G, Hsieh JC, Hartmann A, Knuechel R, Rosenthal A and Pilarsky C. (2003). *J. Pathol.*, **201**, 204–212.
Wolf G, Elez R, Doermer A, Holtrich U, Ackermann H, Stutte HJ, Altmannsberger HM, Rubsamen-Waigmann H and Strebhardt K. (1997). *Oncogene*, **14**, 543–549.
Xu XR, Huang J, Xu ZG, Qian BZ, Zhu ZD, Yan Q, Cai T, Zhang X, Xiao HS, Qu J, Liu F, Huang QH, Cheng ZH, Li NG, Du JJ, Hu W, Shen KT, Lu G, Fu G, Zhong M, Xu SH, Gu WY, Huang W, Zhao XT, Hu GX, Gu JR, Chen Z and Han ZG. (2001). *Proc. Natl. Acad. Sci. USA*, **98**, 15089–15094.
Yun K, Jinno Y, Sohda T, Niikawa N and Ikeda T. (1998). *J. Pathol.*, **185**, 91–98.

Research Article

CpG Island Methylator Phenotype Is a Strong Determinant of Poor Prognosis in Neuroblastomas

Masanobu Abe,[1,2] Miki Ohira,[3] Atsushi Kaneda,[1] Yukiko Yagi,[1] Seiichiro Yamamoto,[4] Yoshihiro Kitano,[5] Tsuyoshi Takato,[2] Akira Nakagawara,[3] and Toshikazu Ushijima[1]

[1]Carcinogenesis Division, National Cancer Center Research Institute; [2]Department of Oral and Maxillo Facial Surgery, University of Tokyo Graduate School of Medicine; [3]Biochemistry Division, Chiba Cancer Center Research Institute; [4]Information Division, Research Center for Cancer Prevention and Screening, National Cancer Center; and [5]Department of Pediatric Surgery, National Center for Child Health and Development, Tokyo, Japan

Abstract

Neuroblastoma, one of the most common pediatric solid tumors, is characterized by two extreme disease courses, spontaneous regression and life-threatening progression. Here, we conducted a genome-wide search for differences in DNA methylation that distinguish between neuroblastomas of the two types. Three CpG islands (CGI) and two groups of CGIs were found to be methylated specifically in neuroblastomas with a poor prognosis. By quantitative analysis of 140 independent cases, methylation of all the five CGI (groups) was shown to be closely associated with each other, conforming to the CpG island methylator phenotype (CIMP) concept. The presence of CIMP was sensitively detected by methylation of the *PCDHB* CGIs and associated with significantly poor survival (hazard ratio, 22.1; 95% confidence interval, 5.3-93.4; $P < 0.0001$). Almost all cases with N-*myc* amplification (37 of 38 cases) exhibited CIMP. Even in 102 cases without N-*myc* amplification, the presence of CIMP (30 cases) strongly predicted poor survival (hazard ratio, 12.4; 95% confidence interval, 2.6-58.9; $P = 0.002$). Methylation of *PCDHB* CGIs, located in their gene bodies, did not suppress gene expression or induce histone modifications. However, CIMP was significantly associated with methylation of promoter CGIs of the *RASSF1A* and *BLU* tumor suppressor genes. The results showed that neuroblastomas with CIMP have a poor prognosis and suggested induction of silencing of important genes as an underlying mechanism. (Cancer Res 2005; 65(3): 828-34)

Introduction

Epigenetic abnormalities, especially alterations in DNA methylation, are intimately involved in development of various human tumors (1). Aberrant methylation of promoter CpG islands (CGI) causes inactivation of tumor suppressor genes. Genomic instability is caused by genomic hypomethylation and is associated with hypermethylation (2, 3). Identification of epigenetic abnormalities in human cancers is expected to lead not only to discovery of novel disease mechanisms but also to development of new diagnostic markers. Therefore, we previously developed a genome-wide scanning method, methylation-sensitive representational difference analysis (MS-RDA), for detecting differences in DNA methylation (4, 5). This technique analyzes unmethylated, CpG-rich regions of the genome and has already identified genes silenced in human lung, stomach, breast, and pancreatic cancers (6–9).

Neuroblastoma derived from primitive cells of the sympathetic nervous system is one of the most common solid tumors in childhood, characterized by two extreme disease courses, spontaneous regression, and life-threatening progression (10, 11). The clinical outcome is associated with disease stage, age at diagnosis, histologic classification, N-*myc* amplification, DNA ploidy, and *TrkA* overexpression (10–12). These characteristics are therefore used to classify cases into low-, intermediate-, and high-risk groups. However, especially in the cases with intermediate risk, prediction of prognosis and therapeutic decision-making are still difficult, and development of new markers is an urgent priority. Moreover, the molecular bases underlying the two distinct clinical courses are still unknown, and their clarification is needed to allow development of novel therapeutics.

In the present study, considering the major involvement of epigenetic machinery in embryonic development (13, 14), we searched for differences in DNA methylation between neuroblastomas with a good prognosis and counterparts with a poor prognosis by MS-RDA.

Materials and Methods

Tissue Samples and Cell Lines. Tumor samples were obtained from 145 nonrecurrent cases between 1995 and 1999 and were used under approval of institutional review boards. The mean age at initial diagnosis was 27 months (range, 0-216 months). Their clinical stages were determined according to the International Neuroblastoma Staging System, and 40, 17, 20, 60, and 8 cases belonged to stages I, II, III, IV, and IVS, respectively. Normal adrenal medulla tissue was collected from a case undergoing nephrectomy for a renal cancer. Neuroblastoma cell lines were obtained from the American Type Culture Collection (Manassas, VA), the Japanese Collection of Research Bioresources (Tokyo, Japan), and the RIKEN Bio Resource Center (Tsukuba, Japan). GANB was established by A.N. and normal human bronchial epithelial cells were purchased from Cambrex (East Rutherford, NJ). High molecular weight DNA and total RNA were extracted as previously described (7). Total RNAs of brain and adrenal glands were purchased from Clontech (Palo Alto, CA).

MS-RDA and Database Search. MS-RDA was done as previously described (4, 5). Genomic DNA of primary neuroblastomas with a good prognosis (cases 92, 98, 104, 112, and 148) and neuroblastoma cell lines established from cases with a poor prognosis (CHP134, IMR32, GANB, NGP, and TGW) were digested with *Hpa*II, and then two pooled DNA samples were prepared. Although use of cell lines is highly recommended for MS-RDA (5), no cell lines were available for neuroblastomas with a good prognosis, and therefore we used the primary samples. To isolate CGIs that were hypermethylated in the latter, the cell line pool was used as the tester, and the primary tumor pool as the driver. MS-RDA in the opposite direction

Note: Supplementary data for this article are available at Cancer Research online (http://cancerres.aacrjournals.org/).

Requests for reprints: Toshikazu Ushijima, 5-1-1 Tsukiji, Chuo-ku, Tokyo 104-0045, Japan. Phone: 133-547-5240; Fax: 135-565-1753; E-mail: tushijim@ncc.go.jp.

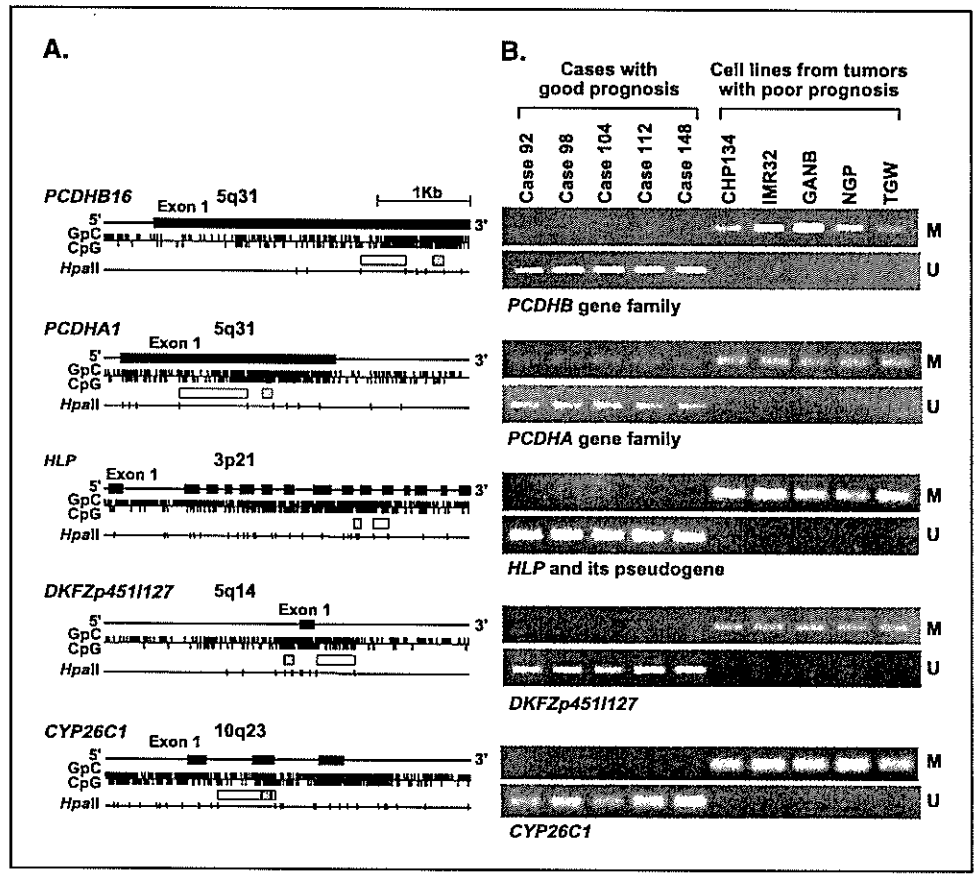

Figure 1. Five CGIs isolated by MS-RDA and their methylation statuses in the samples used for MS-RDA. *A*, genomic structures of the five CGIs. GpC, CpG, and *Hpa*II recognition sites (5′-CCGG-3′) are shown by ticks. *Closed boxes*, exons; *open boxes*, clones isolated by MS-RDA; *shaded boxes*, regions analyzed by MSP. *B*, methylation statuses analyzed by MSP. *M*, MSP using primers specific to methylated DNA; *U*, MSP using primers specific to unmethylated DNA. All the five CGIs were found to be differentially methylated between the two groups used for MS-RDA.

was also done. For each series of MS-RDA, 96 clones were analyzed for redundancy, and nonredundant clones were sequenced. Their genomic origins were examined using BLASTN software http://www.ncbi.nlm.nih.gov/BLAST/).

Sodium Bisulfite Modification and Methylation-Specific PCR. One microgram of DNA underwent sodtlbium bisulfite modification (15), and was suspended in 20 μL of TE buffer. For methylation-specific PCR (MSP), 1 μL of the solution was used for PCR with primers specific to methylated or unmethylated sequences. Using DNA from normal human bronchial epithelial and DNA methylated with *Sss*I methylase, annealing temperatures specific for methylated and unmethylated primers were determined. Quantitative MSP was done separately for methylated DNA molecules and for unmethylated DNA molecules. Standard DNA was prepared by cloning PCR products amplified by methylated and unmethylated primers into a vector, respectively. The numbers of methylated and unmethylated molecules in a test sample were determined by comparing their amplification with those of standard samples containing 10 to 10^6 molecules. The "methylation index" was calculated as the fraction of methylated molecules in the total DNA molecules (no. methylated molecules + no. unmethylated molecules). Each sample was analyzed twice, blind to clinical information, and high reproducibility was confirmed (correlation coefficient = 0.98).

The *protocadherin* β (*PCDHB*) family consists of 16 genes with single exons and three pseudogenes on 5q31, and their CGIs are located in the gene bodies. MSP primers were designed to recognize 17 of the 19 members (all except for the *PCDHB1* gene and the *PCDHB19* pseudogene). The *protocadherin* α (*PCDHA*) family consists of 15 genes and one pseudogene having unique first exons and shared exons 2 to 4 on 5q31, and their CGIs are located in exon 1. MSP primers were designed to recognize 13 of the 16 members (all except for the *PCDHAC1* and *PCDHAC2* genes and the *PCDHA14* pseudogene). The *hepatocyte growth factor-like protein* (*HLP/MSP/MST1*) gene is highly homologous to *macrophage stimulating, pseudogene 9* (*MSTP9*), and MSP primers were designed to recognize both of these. For *DKFZp451I127*, *FLJ37440*, *Zinc finger protein 297* (*ZNF297*), and *Cytochrome p450 CYP26C1* (*CYP26C1*), MSP primers were designed to recognize each of them specifically. The primers and PCR conditions are shown in Supplementary Table 1.

Semiquantitative and Quantitative Reverse Transcription-PCR. cDNA was synthesized from 3 μg of total RNA treated with DNase using a Superscript II kit (Invitrogen Co., Carlsbad, CA). For semiquantitative reverse transcription-PCR (*PCDHB1-PCDHB15*), multiple cycles of PCR were tested for each gene, and numbers giving a wide dynamic range were determined. The primers and PCR conditions are shown in Supplementary Table 2. For quantitative reverse transcription-PCR (*PCDHB16*), the number of cDNA molecules was determined by quantitative PCR, as in quantitative MSP, and the copy number was normalized to that of *GAPDH*.

Chromatin Immunoprecipitation Assay. From 1×10^6 cells, DNA/histone complexes were immunoprecipitated, and DNA was eluted in 30 μL of TE after reversing cross-linking. Copy numbers of DNA molecules of the *PCDHB16* exon, *RASSF1A* promoter, and *GAPDH* promoter in 1 L of the eluate were determined by quantitative PCR (primer sequences in Supplementary Table 3), and normalized to the copy numbers in the input. Anti-acetyl-histone H3 antibody (AcH3) and anti-dimethylated-histone H3 (lysine 9; MetH3K9) were purchased from Cell Signalling (Beverly, MA).

Statistical Analysis. Associations between methylation levels among CGI groups were examined using the Pearson correlation coefficient and Fisher's exact test. Survival time was measured from the date of initial diagnosis to the date of death or last contact. Kaplan-Meier analysis and log-rank tests were done to compare survival between the groups defined by methylation levels. Hazard ratio (HR) between groups and dose-response relationships between methylation levels and survival were estimated by the Cox proportional hazard model. Kaplan-Meier curves were drawn with the help of Aabel software (Gigawiz. Ltd. Co., Tulsa, OK) and other analyses were conducted using SAS version 8.2 (SAS Institute, Inc., Cary, NC).

Results

Genome-Scanning for Differentially Methylated CpG Islands. MS-RDA was done using five primary neuroblastomas with a good prognosis and five neuroblastoma cell lines established from cases with a poor prognosis. Seven DNA fragments, derived from CGIs of *PCDHB16*, *PCDHA1*, *HLP*, *DKFZp451I127*, *FLJ37440*, *ZNF297*, and *CYP26C1*, were isolated as methylated in the latter samples. No DNA fragments were isolated as methylated in the former samples. Methylation statuses of (i) 17 CGIs of the *PCDHB* family (detailed structure in Supplementary Fig. 1), (ii) 13 CGIs of the *PCDHA* family, (iii) *HLP* and its pseudogene, and (iv) other four unique CGIs were examined by MSP. This revealed that the *PCDHB* family (5q31), the *PCDHA* family (5q31), *HLP* (3p21) and its pseudogene (1p36), *DKFZp451I127* (5q14), and *CYP26C1* (10q23) were specifically methylated in the latter samples (Fig. 1*A* and *B*).

Close Association between Methylation and Poor Prognosis in 140 Independent Primary Samples. To analyze the significance of the differential methylation of the above five CGI (groups) in primary neuroblastomas, 140 primary samples, all different from the initial five samples, were analyzed by quantitative MSP. When distributions of methylation indices were analyzed (Fig. 2), a clear bimodal distribution was observed for (i) the CGI group in the *PCDHB* family (17 CGIs), (ii) the CGIs of *HLP* and its pseudogene, and (iii) the *CYP26C1* CGI. The results thus indicated that the cases could be classified into two groups, one with high methylation and the other with low methylation. The dose-response relationships between high *PCDHB* methylation and poor prognosis were analyzed by the Cox proportional model using the methylation index as a continuous value, and the association was confirmed with a trend $P < 0.0001$. Normal adrenal medulla had a methylation index of 4%.

According to the bimodal distribution, the effect of high methylation was assessed by dichotomous groups. For the *PCDHB* family, cutoff values of 30%, 40%, 50%, 60%, 70%, and 80% were tested, and HRs of 16.8 [95% confidence interval (95% CI), 4.0-70.9], 22.1 (95% CI, 5.3-93.4; Fig. 3), 13.1 (95% CI, 4.5-37.9), 9.1 (95% CI, 3.8-23.4), 7.0 (95% CI, 3.1-15.8), and 7.8 (95% CI, 3.4-17.6), respectively, were obtained ($P < 0.001$ for all cutoff values). This showed that cases can be classified into two groups with distinct prognoses, and we adopted a cutoff value of 40%, which gave the highest HR, for convenience in the following analysis.

The dose-response relationships were also confirmed for other four CGI (groups), *PCDHA* ($P = 0.004$), *HLP* ($P < 0.0001$), *DKFZp451I127* ($P = 0.02$), and *CYP26C1* ($P < 0.0001$). Cutoff values were similarly tested, and those for *PCDHA*, *HLP*, *DKFZp451I127*, and *CYP26C1* were set at 80%, 10%, 20%, and 70%, respectively, with HRs of 5.7 (95%CI, 1.4-24.0; $P = 0.07$), 21.7 (95% CI, 5.1-91.4; $P < 0.0001$), 3.2 (95% CI, 1.0-10.5; $P = 0.045$), and 8.7 (95% CI, 4.1-18.1; $P < 0.0001$), respectively (Fig. 3).

Existence of the CpG Island Methylator Phenotype in Neuroblastomas. Methylation of the different CGI (groups) had shown close associations with each other (Table 1). When correlation was analyzed as a continuous value, Pearson correlation coefficients between *PCDHB* and *PCDHA*, *HLP*, *DKFZp451I127* and *CYP26C1* were 0.55, 0.70, 0.26 and 0.77, respectively. This showed that multiple CGIs were simultaneously methylated in

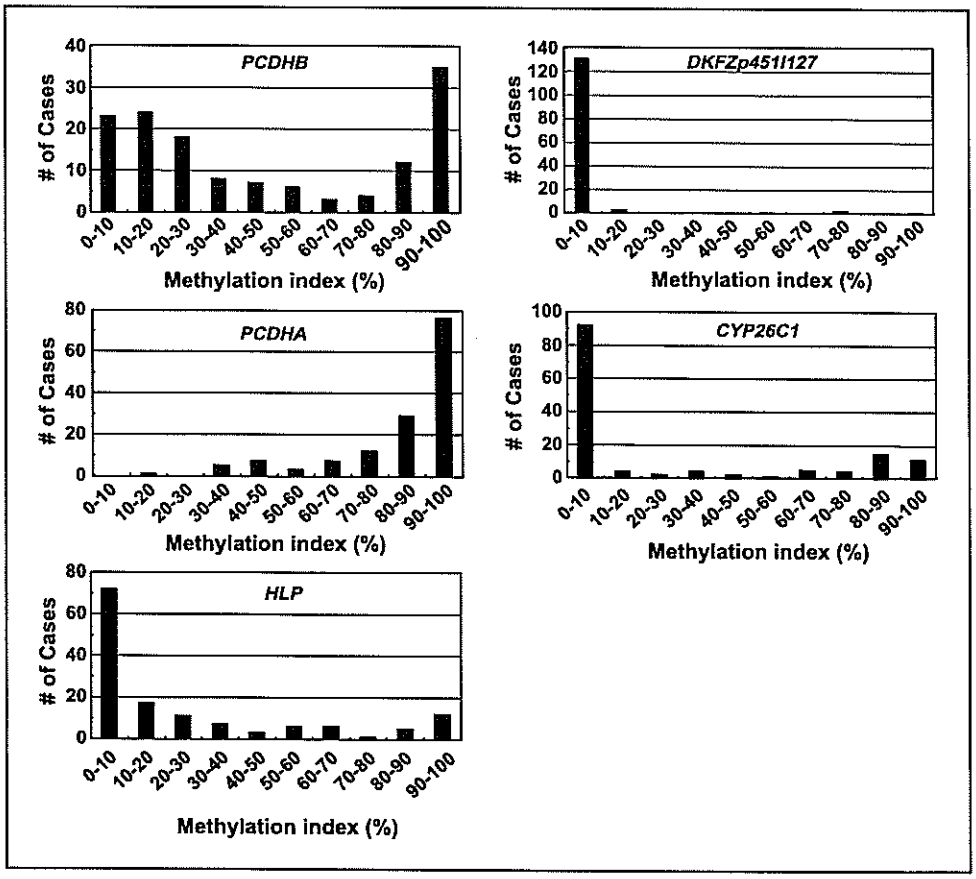

Figure 2. The distribution of methylation indices among the 140 cases analyzed: (*i*) 17 CGIs of the *PCDHB* family, (*ii*) 13 CGIs of the *PCDHA* family, (*iii*) CGIs of *HLP* and its pseudogene, (*iv*) *DKFZp451I127*, and (*v*) *CYP26C1*.

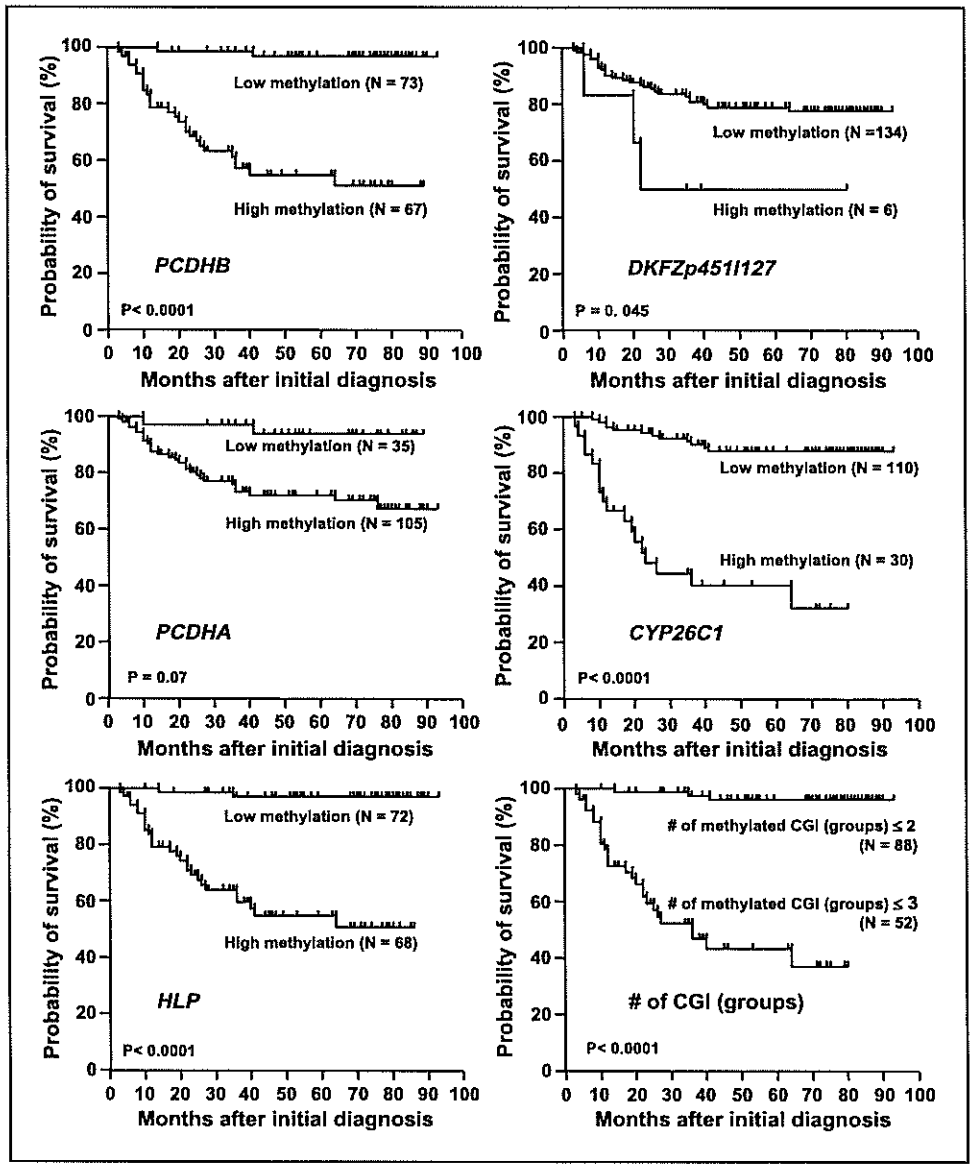

Figure 3. Predictive powers of methylation of the five CGI (groups) identified, and their multiple methylation: (*i*) 17 CGIs of the *PCDHB* family, (*ii*) 13 CGIs of the *PCDHA* family, (*iii*) CGIs of *HLP* and its pseudogene, (*iv*) *DKFZp451I127*, (*v*) *CYP26C1*, and (*vi*) methylation of three of these or more were analyzed by the Kaplan-Meier method using 140 primary samples. The *PCDHB* family, *HLP*, *DKFZp451I127*, *CYP26C1*, and methylation of multiple CGI (groups) had significant influence on survival.

neuroblastomas with a poor prognosis (Supplementary Fig. 2*A*). The simultaneous methylation of (i) 17 CGIs of the *PCDHB* family, (ii) 13 CGIs of the *PCDHA* family, (iii) CGIs of *HLP* and its pseudogene, (iv) *DKFZp451I127* CGI, and (v) *CYP26C1* CGI conformed with the concept of the CpG island methylator phenotype (CIMP; ref. 16).

Associations between CIMP and poor prognosis were examined by defining CIMP as cases with methylation of two CGI (groups) or more, those with three or more, those with four or five, and those with five. When CIMP was defined as cases with methylation of three CGI (groups) or more, the largest association with poor prognosis was observed, with a HR of 25.4 (95% CI, 7.6-84.5; Fig. 3). However, the HR (22.1) given by 17 CGIs of the *PCDHB* gene family approximated to this, and the *PCDHB* methylation level closely correlated with the number of methylated CGI (groups; Supplementary Fig. 2*B*). Therefore, for simplicity of analysis, we defined CIMP in neuroblastomas on the basis of high methylation of the *PCDHB* family, tentatively with a cutoff value of 40%.

Predictive Power of CIMP, Compared with Known Prognostic Factors. Univariate analyses showed that N-*myc* amplification, low *TrkA* expression, DNA diploidy, and an age no younger than 1 year gave HRs of 9.5 (95% CI, 4.4-20.5), 3.9 (95% CI, 1.7-9.3), 4.2 (95% CI, 1.65-10.8), and 12.3 (95% CI, 3.7-41.7). Cases were stratified by these known factors (Table 2). In those without N-*myc* amplification, CIMP also showed an influence with a HR of 12.4 (95% CI, 2.6-58.9), but almost all cases with N-*myc* amplification (37 of the 38 cases) showed CIMP. It was suggested that cases with N-*myc* amplification were contained in the cases with CIMP. CIMP was independent from *TrkA* overexpression, DNA ploidy, and age at diagnosis. Stage seemed to be a stronger prognostic factor. Notably, even when limited to cases in stages III and IV without N-*myc* amplification, which are classified into the intermediate risk group and clinically important, CIMP gave a HR of 4.8 (95% CI, 1.0-23.0; $P = 0.048$).

Multivariate analyses were finally done taking all the five known prognostic factors into account. Although CIMP gave a HR of 5.0 (95% CI, 0.47-52.7), it was not significant ($P = 0.18$), possibly due to limitation in the number of cases.

Table 1. Association between the *PCDHB* methylation and methylation of other CGIs

Variables	Methylation level of *PCDHB* family gene		*P**
	High (≥40%)	Low (<40%)	
No. cases (n = 140)	67	73	
Methylation of CGIs outside promoter regions (n = 140)			
PCDHA gene family (exon 1)†	65/67	41/73	<0.0001
HLP (exons 2-13)‡	52/67	16/73	<0.0001
CYP26C1 (exon 2)§	30/67	0/73	<0.0001
p41Arc (intron 8)	1/67	1/73	0.48
SIM2 (exon 2)	0/67	0/73	
Methylation of CGIs in promoter regions (n = 140)			
DKFZp451I127‖	6/67	0/73	0.011
RASSF1A	51/67	10/73	<0.0001
BLU	25/67	3/73	<0.0001
p16	0/67	0/73	
hMLH1	0/67	0/73	
PCDHB1	0/67	0/73	
TAF7	0/67	0/73	
p41Arc	0/67	0/73	
SIM2	0/67	0/73	

*Fisher's exact test.
†Boundaries for high methylation and low methylation of *PCDHA* gene family were set at 80% of the methylation index.
‡Boundaries for high methylation and low methylation of *HLP* were set at 10% of the methylation index.
§Boundaries for high methylation and low methylation of *CYP26C1* were set at 70% of the methylation index.
‖Boundaries for high methylation and low methylation of *DKFZp451I127* were set at 20% of the methylation index.

Effects of PCDHB Methylation on Gene Expression and Chromatin Structure. The CGIs of the *PCDHB* family were located in their gene bodies, whose methylation generally does not block gene transcription (17). The actual effects of methylation on expression were examined for 16 genes of the *PCDHB* family using 10 primary neuroblastomas with low methylation and five primary neuroblastomas with high methylation. The methylation was not associated with loss of expression (a representative result is shown in Fig. 4*A*). The effect of methylation of the *PCDHB16* CGI on the histone modification was further examined by chromatin immunoprecipitation assay. It was found that DNA methylation of the *PCDHB16* CGI did not induce histone H3 lysine 9 methylation or histone H3 deacetylation (data not shown).

Association between CIMP and Promoter Methylation. High methylation of *PCDHB* CGIs, a sensitive surrogate marker of CIMP in neuroblastomas, did not repress gene expression or induce histone modification. This indicated that CIMP is involved in the poor prognosis of neuroblastomas by causing methylation of promoter CGIs, although it is known that promoter CGIs are resistant to *de novo* methylation (18, 19).

Among the five CGI (groups) identified in this study, only that of *DKFZp451I127* was located in a promoter region. Although its methylation was infrequent, the methylation was observed only in neuroblastomas with CIMP (Table 1), and was associated with expression loss (Fig. 4*B*). To make the association clearer, methylation statuses were analyzed for eight additional CGIs in promoter regions. It was shown that methylation of promoter CGIs of *RASSF1A* (3p21) and *BLU* (3p21) was far more frequently observed in neuroblastomas with CIMP (Table 1, $P < 0.0001$). At the same time, there was a preference for CGIs affected by CIMP among CGIs in promoter regions, and also among those outside promoter regions (Table 2).

Discussion

Extensive methylation of multiple CGIs, conforming with the concept of CIMP, was here found specifically present in neuroblastomas with a poor prognosis and could be sensitively detected by focusing on the *PCDHB* family. *PCDHB* methylation did not suppress gene expression or induce histone modification. However, CIMP was associated with promoter methylation of *RASSF1A* and *BLU* genes and one of the mechanisms underlying the poor prognosis of neuroblastomas seemed to be silencing of these and possibly other tumor suppressor genes and genes important for differentiation.

CIMP was originally identified in colon cancers (16), but there has been some dispute over its presence (20). The clear correlation between CIMP and a poor prognosis found here for neuroblastomas was unequivocal and presumably reflects an intrinsic tendency for methylation of CGIs. This is because, first, neuroblastomas have a much shorter history than colon cancers, and the accumulated number of methylated CGIs in neuroblastomas is expected to parallel the speed of occurrence of

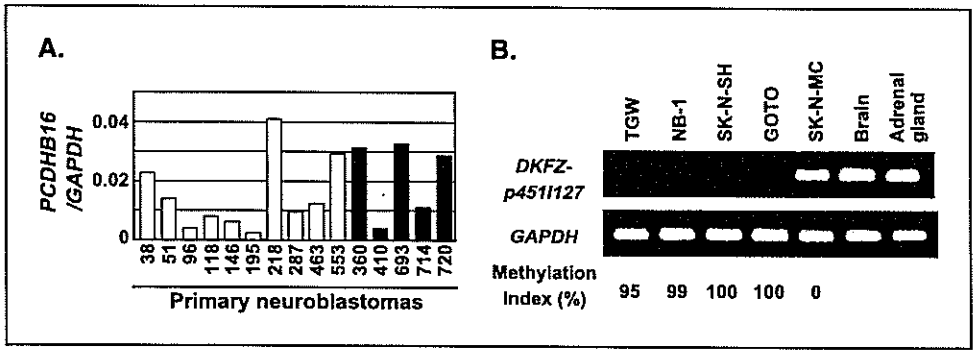

Figure 4. Effects of methylation of the *PCDHB* family and *DKFZp451I127* on gene expression. *A*, *PCDHB16* expression was analyzed by quantitative RT-PCR in 10 primary samples with low methylation (*open columns*) and five primary samples with high methylation (*closed columns*), and no difference was observed between the two groups. *B*, silencing of *DKFZp451I127* by methylation of its promoter CGI. The CGI was methylated in four cell lines, TGW, NB-1, SK-N-SH, and GOTO, whereas it was unmethylated in one cell line, SK-N-MC. *DKFZp451I127* was expressed in SK-N-MC, but not expressed at all in the four cell lines with the promoter methylation.

Table 2. HRs of death by *PCDHB* methylation status in subgroup of known prognostic factors

Stratified by		*PCDHB* methylation	No. cases	No. deaths	HR* (95% CI)	$P^{\dagger}$
Overall (n = 140)		High	67	1	22.1 (5.3-93.4)	< 0.0001
		Low	73	2	1	
N-*myc* amplification (n = 140)	No	High	30	8	12.4 (2.6-58.9)	0.002
		Low	72	2	1	
	Yes	High	37	20	NE	—
		Low	1	0		
TrkA overexpression (n = 130)	Yes	High	20	6	18.3 (2.2-152.6)	0.007
		Low	49	1	1	
	No	High	40	19	NE	
		Low	21	0		
DNA ploidy (n = 125)	Aneuploid	High	17	5	18.3 (2.1-156.7)	0.008
		Low	49	1	1	
	Diploid	High	38	17	NE	
		Low	21	0		
Clinical stages (n = 140)	Stages I, II, and IVS	High	8	0	NE	—
		Low	52	0		
	Stages III and IV	High	59	28	7.4 (1.8-31.3)	0.006
		Low	21	2	1	
Age at diagnosis (n = 140)	<1	High	11	3	NE	
	≥1	Low	59	0		
		High	56	25	4.5 (1.1-18.9)	0.043
		Low	14	2	1	

*HR of death for a case with high *PCDHB* methylation compared with a case with low methylation. NE shows not estimable due to no events in at least one category.
†Significance level for a high *PCDHB* methylation to low methylation using Cox proporitonal model.

methylation. Second, methylation of the *PCDHB* family did not affect gene expression, and there should have been no selection of cells with the *PCDHB* methylation, in contrast to the case of promoter methylation of tumor suppressor genes. Investigation into the mechanism of the intrinsic tendency for methylation of multiple CGIs is necessary. Furthermore, alleviation of the intrinsic tendency could block progression of neuroblastomas and have potential therapeutic value.

Among the six CGI (groups) outside promoter regions analyzed here, CIMP in neuroblastomas preferentially affected four CGI (groups); those of the *PCDHB* family, the *PCDHA* family, *HLP*, and *CYP26C1*. Unexpectedly, three CGIs that are known to be frequently methylated in human colon cancers with CIMP, MINT1, MINT2, and MINT17 (16) were not methylated in neuroblastoma cell lines (data not shown). Among the nine CGIs in promoter regions analyzed, CIMP in neuroblastomas affected only three, those of *RASSF1A*, *BLU*, and *DKFZp451I127*. The nine CGIs were selected based upon previous reports as tumor suppressor genes (*RASSF1A*, *BLU*, *p16*, and *hMLH1*; refs. 21–23), the chromosomal location flanking the *PCDHB* family (*PCDHB1* and *TAF7*), our previous report on the fidelity in inheriting methylation patterns (*p41Arc* and *SIM2*; ref. 19), and the findings here (*DKFZp451I127*). Because gene expression and possibly chromatin structures affect the frequency of *de novo* methylation (24, 25), the available data suggest that CGIs useful to sensitively detect CIMP might vary according to the tumor type.

The influence of CIMP on prognosis was here found to be comparable to that of the currently most reliable marker, N-*myc* amplification, and stronger than *TrkA* overexpression and DNA ploidy on univariate analysis. Subgroup analysis showed that the influence was independent of *TrkA* overexpression, DNA ploidy and age at diagnosis and CIMP had influence even in cases without N-*myc* amplification and in advanced stages. These points strongly indicated CIMP to be a promising new prognostic marker. However, the cutoff values adopted here are tentative, and the HRs obtained could have been overestimated. A validation study using independent samples is necessary for further evaluation. The fact that cases with CIMP contained almost all the cases with N-*myc* amplification suggested that a common molecular mechanism caused both alterations, or that CIMP may lead to N-*myc*

amplification. Whatever the case, the findings might provide clues to molecular mechanisms of neuroblastoma development.

In summary, the present study showed that CIMP is present specifically in neuroblastomas with poor prognosis and that can be sensitively detected by focusing on *PCDHB* methylation. CIMP seems to be a promising new prognostic marker, and its evaluation and investigations into the mechanisms underlying CIMP in neuroblastomas seem warranted.

Acknowledgments

Received 7/27/2004; revised 11/14/2004; accepted 11/24/2004.

Grant support: Grant-in-aid for the Third-term Cancer Control Strategy Program from the Ministry of Health, Labour, and Welfare, Japan and Research Resident Fellowship from the Foundation for Promotion of Cancer Research (M. Abe).

The costs of publication of this article were defrayed in part by the payment of page charges. This article must therefore be hereby marked advertisement in accordance with 18 U.S.C. Section 1734 solely to indicate this fact.

We thank Drs. E. Okochi-Takada and G. S. Goldberg for critical reading of the article and the institutions for participation in the collection of clinical materials.

References

1. Jones PA, Baylin SB. The fundamental role of epigenetic events in cancer. Nat Rev Genet 2002;3:415–28.
2. Chen RZ, Pettersson U, Beard C, Jackson-Grusby L, Jaenisch R. DNA hypomethylation leads to elevated mutation rates. Nature 1998;395:89–93.
3. Kondo Y, Kanai Y, Sakamoto M, et al. Genetic instability and aberrant DNA methylation in chronic hepatitis and cirrhosis-A comprehensive study of loss of heterozygosity and microsatellite instability at 39 loci and DNA hypermethylation on 8 CpG islands in microdissected specimens from patients with hepatocellular carcinoma. Hepatology 2000;32:970–9.
4. Ushijima T, Morimura K, Hosoya Y, et al. Establishment of methylation-sensitive-representational difference analysis and isolation of hypo- and hypermethylated genomic fragments in mouse liver tumors. Proc Natl Acad Sci U S A 1997;94:2284–9.
5. Kaneda A, Takai D, Kaminishi M, Okochi E, Ushijima T. Methylation-sensitive representational difference analysis and its application to cancer research. Ann N Y Acad Sci 2003;983:131–41.
6. Takai D, Yagi Y, Wakazono K, et al. Silencing of *HTR1B* and reduced expression of *EDN1* in human lung cancers, revealed by methylation-sensitive representational difference analysis. Oncogene 2001; 20:7505–13.
7. Kaneda A, Kaminishi M, Yanagihara K, Sugimura T, Ushijima T. Identification of silencing of nine genes in human gastric cancers. Cancer Res 2002;62:6645–50.
8. Miyamoto K, Asada K, Fukutomi T, et al. Methylation-associated silencing of heparan sulfate *D-glucosaminyl 3-O-sulfotransferase-2* (*3-OST-2*) in human breast, colon, lung and pancreatic cancers. Oncogene 2003;22:274–80.
9. Hagihara A, Miyamoto K, Furuta J, et al. Identification of 27 5′ CpG islands aberrantly methylated and 13 genes silenced in human pancreatic cancers. Oncogene 2004;23:8705–10.
10. Brodeur GM. Neuroblastoma: biological insights into a clinical enigma. Nat Rev. Cancer 2003;3:203–16.
11. Schwab M, Westermann F, Hero B, Berthold F. Neuroblastoma: biology and molecular and chromosomal pathology. Lancet Oncol 2003;4:472–80.
12. Nakagawara A, Arima-Nakagawara M, Scavarda NJ, et al. Association between high levels of expression of the *TRK* gene and favorable outcome in human neuroblastoma. N Engl J Med 1993;328:847–54.
13. Jaenisch R, Bird A. Epigenetic regulation of gene expression: how the genome integrates intrinsic and environmental signals. Nat Genet 2003;33:245–54.
14. Li E. Chromatin modification and epigenetic reprogramming in mammalian development. Nat Rev Genet 2002;3:662–73.
15. Kaneda A, Kaminishi M, Sugimura T, Ushijima T. Decreased expression of the seven ARP2/3 complex genes in human gastric cancers. Cancer Lett 2004; 212:203–10.
16. Toyota M, Ahuja N, Ohe-Toyota M, et al. CpG island methylator phenotype in colorectal cancer. Proc Natl Acad Sci U S A 1999;96:8681–6.
17. Gonzalgo ML, Hayashida T, Bender CM, et al. The role of DNA methylation in expression of the *p19/p16* locus in human bladder cancer cell lines. Cancer Res 1998;58:1245–52.
18. Nguyen C, Liang G, Nguyen TT, et al. Susceptibility of nonpromoter CpG islands to *de novo* methylation in normal and neoplastic cells. J Natl Cancer Inst 2001; 93:1465–72.
19. Ushijima T, Watanabe N, Okochi E, et al. Fidelity of the methylation pattern and its variation in the genome. Genome Res 2003;13:868–74.
20. Yamashita K, Dai T, Dai Y, Yamamoto F, Perucho M. Genetics supersedes epigenetics in colon cancer phenotype. Cancer Cell 2003;4:121–31.
21. Agathanggelou A, Dallol A, Zochbauer-Muller S, et al. Epigenetic inactivation of the candidate 3p21.3 suppressor gene *BLU* in human cancers. Oncogene 2003; 22:1580–8.
22. Takita J, Hayashi Y, Nakajima T, et al. The *p16* (*CDKN2A*) gene is involved in the growth of neuroblastoma cells and its expression is associated with prognosis of neuroblastoma patients. Oncogene 1998; 17:3137–43.
23. Harada K, Toyooka S, Maitra A, et al. Aberrant promoter methylation and silencing of the *RASSF1A* gene in pediatric tumors and cell lines. Oncogene 2002; 21:4345–9.
24. De Smet C, Loriot A, Boon T. Promoter-dependent mechanism leading to selective hypomethylation within the 5′ region of gene *MAGE-A1* in tumor cells. Mol Cell Biol 2004;24:4781–90.
25. Richards EJ, Elgin SC. Epigenetic codes for heterochromatin formation and silencing: rounding up the usual suspects. Cell 2002;108:489–500.

Expression profiling using a tumor-specific cDNA microarray predicts the prognosis of intermediate risk neuroblastomas

Miki Ohira,[1,8] Shigeyuki Oba,[2,8] Yohko Nakamura,[1] Eriko Isogai,[1] Setsuko Kaneko,[3] Atsuko Nakagawa,[4] Takahiro Hirata,[5] Hiroyuki Kubo,[5] Takeshi Goto,[5] Saichi Yamada,[6] Yasuko Yoshida,[6] Misa Fuchioka,[7] Shin Ishii,[2] and Akira Nakagawara[1,*]

[1]Division of Biochemistry, Chiba Cancer Center Research Institute, Chiba 260-8717, Japan
[2]Graduate School of Information Science, Nara Institute of Science and Technology, Ikoma 630-0192, Japan
[3]Department of Pediatric Surgery, University of Tsukuba School of Medicine, Tsukuba 305-8575, Japan
[4]Second Department of Pathology, Aichi Medical University, Nagakute 480-1195, Japan
[5]Hisamitsu Pharmaceutical Co. Inc., Tokyo 100-622, Japan
[6]Micro Ceramics Laboratory, R & D Center, NGK Insulators, LTD, Nagoya 467-8530, Japan
[7]Center for Molecular Biology and Cytogenetics SRL Inc., Tokyo 191-0002, Japan
[8]These authors contributed equally to this work.
*Correspondence: akiranak@chiba-cc.jp

Summary

To predict the prognosis of neuroblastoma patients and choose a better therapeutic protocol, we developed a cDNA microarray carrying 5340 genes obtained from primary neuroblastomas and examined 136 tumor samples. We made a probabilistic output statistical classifier that provided a high accuracy in prognosis prediction (89% at 5 years) and a highly reliable method to validate it. Kaplan-Meier analysis indicated that the patients in an intermediate group defined by existing markers are divided by microarray into two further groups with 5 year survivals for 36% and 89% of patients ($p < 10^{-4}$), i.e., with unfavorably and favorably predicted neuroblastomas, respectively. According to these results, we developed a gene subset chip for a clinical tool, for which our classifier exhibited 88% prediction accuracy.

Introduction

Neuroblastoma is one of the most common solid tumors in children and originates from the sympathoadrenal lineage of the neural crest (Bolande, 1974). Its clinical behaviors are heterogeneous. The tumor, when developed in infants, frequently regresses spontaneously by inducing differentiation and/or programmed cell death. When developed in children over 1 year of age, however, the tumor is often aggressive and acquires resistance to intensive chemotherapy. Although recent progress in therapeutic strategies against advanced neuroblastoma has improved patient survival, long-term outcomes still remain very poor. Furthermore, part of neuroblastomas categorized to the intermediate group (stage 3 or 4 tumors that possess a single copy of the *MYCN* gene) often recurs after complete response to initial therapy. Such differences in the final outcomes of the tumor are considered presumably attributable to differences in genetic and biological abnormalities, which are reflected in the gene and protein expression profiles of the tumor.

The prediction of cancer prognosis is one of the most urgent demands to initiate the treatment of neuroblastoma. As expected from the natural course of neuroblastoma, patient age at diagnosis (over or under 1 year of age) is an important prognostic factor (Evans et al., 1971). Disease stage is also a powerful indicator for neuroblastoma prognosis (Brodeur et al., 1993). Moreover, recent advances in basic research have discovered several molecular markers that are useful in clinical practice, including amplification of the *MYCN* oncogene (Schwab et al., 1983; Brodeur et al., 1984), DNA ploidy (Look et al., 1984; Look et al., 1991), deletion of chromosome 1p (Brodeur et al., 1988), and *TrkA* expression (Nakagawara et al., 1992; Nakagawara et al., 1993). Other indicators also include *telomerase* (Hiyama et al., 1995), *CD44* (Favrot et al., 1993), *pleiotrophin* (Nakagawara et al., 1995), *N-cadherin* (Shimono et al., 2000), *CDC10* (Nagata et al., 2000), and *Fyn* (Berwanger et al., 2002). However, the combinations thereof still frequently fail to predict patient outcome. In the post-genome sequence era, therefore, the advent of new diagnostic tools has been ex-

SIGNIFICANCE

Neuroblastoma is an enigmatic tumor with heterogeneous clinical behaviors including maturation, regression, and growth. Despite recent improvements in the cure rate of many pediatric tumors, the prognosis of advanced neuroblastoma is still poor. In addition, it is usually difficult to predict the prognosis of the intermediate risk group in advanced stages without *MYCN* amplification. Through our supervised machine learning and highly reliable statistical validation procedure with the 5 year prognosis of the patients, we established a simple, low-cost microarray system carrying top-ranked genes, which exhibited high accuracy (88%) to predict the neuroblastoma prognosis and is highly feasible as a clinical tool.

pected. Recently, the DNA microarray method, applied to comprehensively demonstrate expression profiles of primary neuroblastomas and cell lines, has already identified the following: (1) differences in gene expression between favorable and unfavorable subsets (Yamanaka et al., 2002; Berwanger et al., 2002); and (2) differences in gene expression that occur during retinoic acid-induced neuronal differentiation (Ueda, 2001). However, a study to predict neuroblastoma prognosis with a microarray using a large number of neuroblastoma samples has never been reported. We have recently isolated 5500 genes from the cDNA libraries, which were generated from primary neuroblastomas, part of which has previously been reported (Ohira et al., 2003a; Ohira et al., 2003b). In this study, to identify genes strongly associated with neuroblastoma prognosis and to apply them to make a really practical cDNA microarray for neuroblastoma diagnosis, we constructed an in-house, ink-jet-printed cDNA microarray carrying 5340 genes proper to neuroblastoma and applied it to analyze 136 samples. After selecting genes significantly related to patient prognosis, we made a mini-chip carrying 200 top-ranked genes to apply for the clinic.

There have been many attempts to predict cancer outcome using microarray. A reliable prediction for outcomes of cancer patients naturally demands its reproducibility, and it is quite important to use sound and highly reliable statistical methodologies; a complete crossvalidation analysis without introducing any information leakage and an independent test using new samples are necessary. As Ntzani and Ioannidis (2003) pointed out, however, such a careful methodology has often been ignored in most microarray studies. We here developed a supervised classification method without any information leakage as a statistic tool and demonstrated that the probabilistic output of the analysis defines the molecular signature of neuroblastoma to predict its prognosis. Although the construction of the statistical tool was based on one of the most reliable statistical tests, we also consulted a validation test for an independent experiment examining 50 samples (whose RNAs were prepared in an independent laboratory) by using the mini-chip. The high performance for the outcome prediction by the mini-chip system suggests the high feasibility of developing a clinical tool based on molecular signature.

Results

Neuroblastoma proper cDNA microarray

The whole scheme of our study is summarized in Figure 1. We first constructed a neuroblastoma proper cDNA microarray harboring the spots of 5340 genes on a slide glass by using a ceramics-based ink-jet printing system (the 5340 genes system). This in-house cDNA microarray appeared to have overcome the previous problems caused by pin-spotting, e.g., uneven quantity or shape of individual spots on an array. Ten micrograms each of the total RNA extracted from 136 frozen tissues of primary neuroblastomas were labeled with Cy3 dye. As a common reference, the mixture of the total RNA obtained from four neuroblastoma cell lines with a single copy of *MYCN* (NB69, NBLS, SK-N-AS, and SH-SY5Y) was labeled with Cy5 dye.

We first evaluated the quality of our cDNA microarray, the 5340 genes system. The log Cy3/Cy5 fluorescence ratio of each gene spot was normalized to eliminate intensity-dependent biases. Since the 5340 genes array contains 260 duplicated or multiplicated genes, the expression ratio of such a duplicated gene was represented by the average of multiple spots. Based on estimation performance for missing values (see the Supplemental Data available with this article online) and on reproduction variance of the duplicated genes, the standard deviation for the log ratio of a single gene was sufficiently small, ranging between about 0.2 and about 0.3 (Figure S1A). The scatter plots of the log Cy3/Cy5 fluorescence ratio between duplicated gene spots in the 136 experiments and those between repeated experiments also indicated high reproducibility of spotting and experiment (Figures S1B and S1C). These suggest that the production of and experiments by our cDNA microarray are highly reproducible.

Supervised classification

To develop a statistical tool that predicts the prognosis of a new patient with neuroblastoma, we introduced a supervised classification. In the development, we used 136 neuroblastomas, randomly selected tumor samples from the neuroblastoma tissue bank, consisting of 41 stage 1 tumors, 22 stage 2 tumors, 33 stage 3 tumors, 28 stage 4 tumors, and 12 stage 4s tumors. The follow-up duration ranged between 3 and 241 months (median, 56 months, mean, 57.3 months) after diagnosis. The left panel in Figure 2 compiles summary information of each sample, including survival time and important prognosis markers (see Experimental Procedures for details). Since variations in follow-up duration generated noises in the supervised classification, we used patient outcome (dead or alive) at 5 years after diagnosis as the target label to be predicted. Since the outcomes of 40 of 136 samples were unknown at 5 years after diagnosis, data for 96 remaining samples were used subsequently. When we were interested in short-term outcome prediction, the target label was set at 2 years after diagnosis, for which purpose 126 samples out of the 136 samples were used.

We constructed the weighted voting as a supervised classifier after important genes were selected according to pairwise *F* scores. To estimate the prediction accuracy for new data, we consulted leave two out (LTO) analysis, which obtains almost unbiased estimation of prediction accuracy for new data while avoiding overestimation due to information leakage (Figure S2A). Although it is known that the prediction accuracy of a supervised classifier depends on the number of genes to be used (Figure S3), the LTO procedure enables us to optimize it without introducing information leakage, by using a sample left out at the outer loop of the double-loop procedure (see Experimental Procedures). The crossvalidation accuracy for the 5 year prognosis prediction was as high as 88.5% (sensitivity of 86.7% and specificity of 89.4%) (Table 1, "Whole cases"). In the LTO analysis, we selected genes and constructed the corresponding classifier individually for the outcome prediction of each sample. The average number of the selected genes, n, was 30.7. If we applied the same procedure to the short-term (2 year) prediction, the accuracy, sensitivity, and specificity were 89.8%, 88.0%, and 90.2%, respectively (data not shown).

Construction of a probabilistic output

According to the LTO analysis, we can obtain weighted vote values and the corresponding survival rates. After approximat-

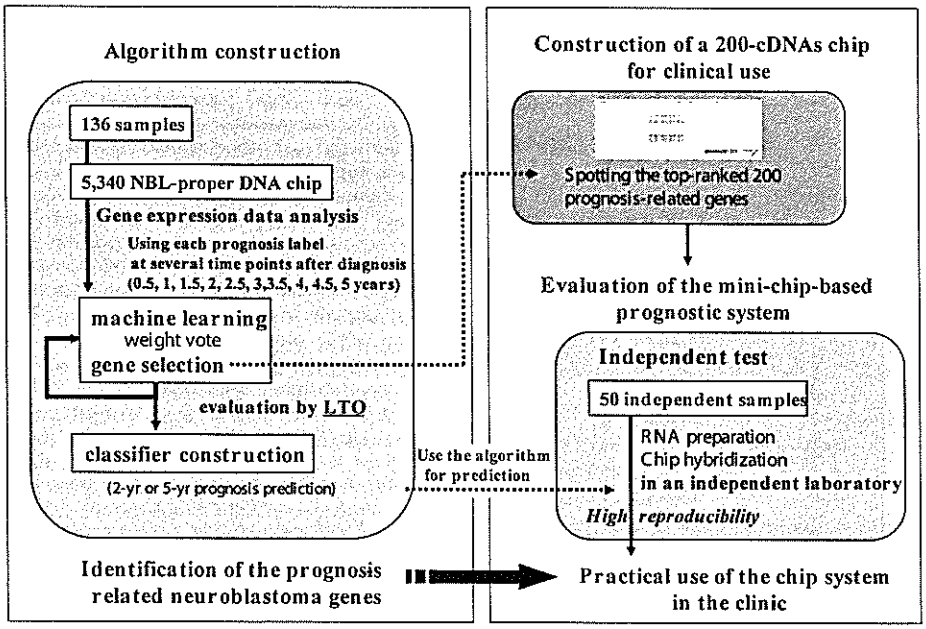

Figure 1. Schematic diagram of this study

ing a nonlinear transformation from weighted vote values to the survival rates, the transformation outputs the reliability of each sample's outcome prediction as a probabilistic output, posterior probability. We suppose each posterior probability, a real number between 0 and 1, corresponds to the expected 5 year survival rate. The right upper panel of Figure 2 shows the predictions for the 136 samples as posterior probabilities. Most of the samples alive at 5 years after diagnosis (blue mark) are found to have posterior values near 1, while most of the dead samples (red mark) have those near 0. It is known that it is difficult to predict the prognosis of neuroblastoma patients of the intermediate risk group (the type II subset: stage 3 or 4, without amplification of *MYCN*), denoted by green area. The posterior values are likely to take intermediate values near 0.5; however, their binarization after being separated by threshold 0.5 shows good accordance with the actual outcome. Frequencies of posterior values for alive and dead samples are shown in the right middle panel. The rate of alive samples among the whole samples, which denotes the actual survival rate, is plotted against each posterior value in the right bottom panel in Figure 2; this panel shows the good correspondence between the posterior value and the survival rate.

Probabilistic outputs are considered to be advantageously useful as compared with conventional binary outputs when used in making a clinical assessment and may be considered identical to them if establishing an appropriate threshold value. The real-valued posterior can be used for categorization into arbitrary number of groups. For example, dividing the posterior values into three by setting thresholds 0.3 and 0.7, we obtain three groups whose survival curves are significantly different from each other; this tertiary categorization provides another definition of intermediate risk group based only on expression patterns (Figure S4).

Comparing the survival curves

Figure 3A shows survival curves for favorable and unfavorable patients predicted by the classifier with a binary threshold (0.5). The 5 year survival rate for the former (n = 98) was as good as 94%, while that for the latter (n = 38) was as poor as 33% ($p < 10^{-5}$). When 70 sporadic neuroblastomas were evaluated after excluding the tumors found by mass screening, the 5 year survival rate for the former (n = 40) was 85%, while that for the latter (n = 30) was 20% ($p < 10^{-5}$) (Figure 3B). To further evaluate the efficiency of our system, we calculated the posterior value for the intermediate subset of neuroblastoma (type II), whose prognosis is usually difficult to predict. As shown in Figure 3C, the survival curves were significantly categorized into two groups. The 5 year survival rate of patients who were predicted as favorable was 89%, while that for unfavorable patients was 36% ($p = 0.000067$). Since the age at diagnosis (≥ 1 year) is currently used as a poor prognostic factor for the type II tumors, we examined the ability of the classifier for the older patients with type II tumors. Even for such patients whose prognosis is difficult to predict, the survival rate (45%) of all 18 patients was divided solely by gene expression into the group with favorable prognosis (n = 10; 73%) and that with poor outcome (n = 8; 13%) (Figure 3D). In addition, if the intermediate risk group was further separated into stage 3 tumor group and stage 4 tumor group, the posterior value was significantly related to the survival, especially for stage 3 tumors (Figure S5). These results suggest that the posterior value obtained by our statistical analysis highly efficaciously allows the classification of patient outcomes, even when the tumor is of the intermediate type.

We further compared our results to existing prognosis markers in Table 1 and found that the supervised microarray analysis showed the best sensitivity-specificity balance among the prognostic factors for predicting the outcome of neuroblastoma. When the classifier is combined with the age at diagnosis, the disease stage (stage 1, 2, or 4s versus stage 3 or 4) and the *MYCN* amplification, accuracy, sensitivity, and specificity increased up to 95.8%, 93.3%, and 97.0%, respectively. Although the currently used markers (age, stage, and *MYCN*)

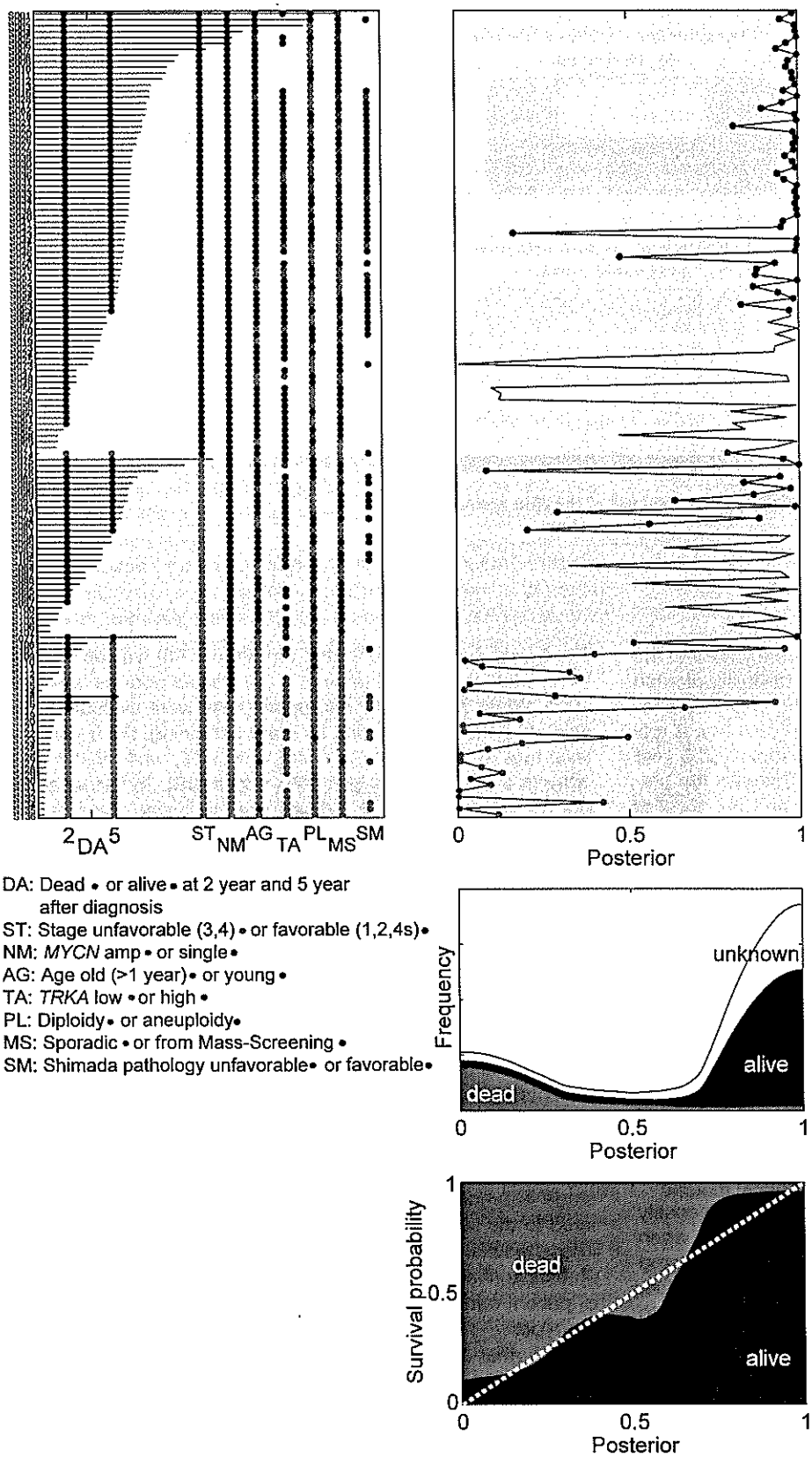

Figure 2. Posterior probability of survival at 5 years

Posterior probability of survival at 5 years for 136 training data samples, output by the leave two out (LTO) crossvalidation without any information leakage. Left panel: Neuroblastoma samples. A red or blue horizontal line denotes survival period after diagnosis for a dead or alive patient, respectively. Red and blue marks denote various clinical properties of patients; see text below the panel for detailed explanation. Background colors show groups determined by stage and *MYCN* amplification status: red, type III, with *MYCN* amplification; green, type II, with single copy of *MYCN* at unfavorable stage (3 or 4); and blue, type I, with single copy of *MYCN* and at favorable stage (1, 2, or 4s). Right upper panel: The LTO crossvalidated prediction (posterior) for each patient; a red or a blue mark denotes that the patient is dead or alive at 5 years, respectively. Right middle panel: Cumulative smooth histogram of posterior probabilities for patients of dead (red), alive (blue), and unknown (white) at 5 years after diagnosis. Right lower panel: The horizontal and vertical axes denote the posterior and the empirical probability of 5 year survival, i.e., the ratio of the smooth histogram values between dead and alive patients, shown in the middle panel, respectively. Because the border between dead and alive samples is close to the white broken line (x = y), the posterior can be regarded as a 5 year survival chance rate.

Table 1. Accuracy of each marker for prognosis prediction (5 years after diagnosis)

	Whole cases				Sporadic cases		Intermediate and old age[a]	
	n	accuracy	sensitivity	specificity	n	accuracy	n	accuracy
Microarray classifier	136	89%	87%	89%	56	82%	14	86%
Age (less than 1 year old)	136	81%	83%	80%	56	71%	14	64%
Stages (1, 2, and 4s)	136	83%	97%	77%	56	84%	14	64%
Shimada classification (unfavorable)	62	87%	78%	89%	25	72%	(n < 10)	—
Hyperdiploidy (aneuploidy)	62	72%	67%	73%	27	56%	(n < 10)	—
MYCN amplification	136	89%	67%	99%	56	80%	14	36%
Microarray + age + stages + MYCN*	136	96%	93%	97%	56	93%	14	86%

Sensitivity/specificity is the rate of unfavorably/favorably predicted samples, i.e., LTO posterior <0.5/>0.5, among actually unfavorable/favorable samples. Microarray classifier, supervised classification based on the microarray data. *By this classifier, all patients with the *MYCN* amplification are predicted as unfavorable, and all patients with a single copy of *MYCN* and at stage 1, 2, or 4s are predicted as favorable. In the remaining intermediate samples (with a single copy of *MYCN* and at stage 3 or 4), the patients with age <1 year are predicted as favorable, and the microarray predictions are applied for those with age >1 year.
[a]Age at diagnosis >1 year.

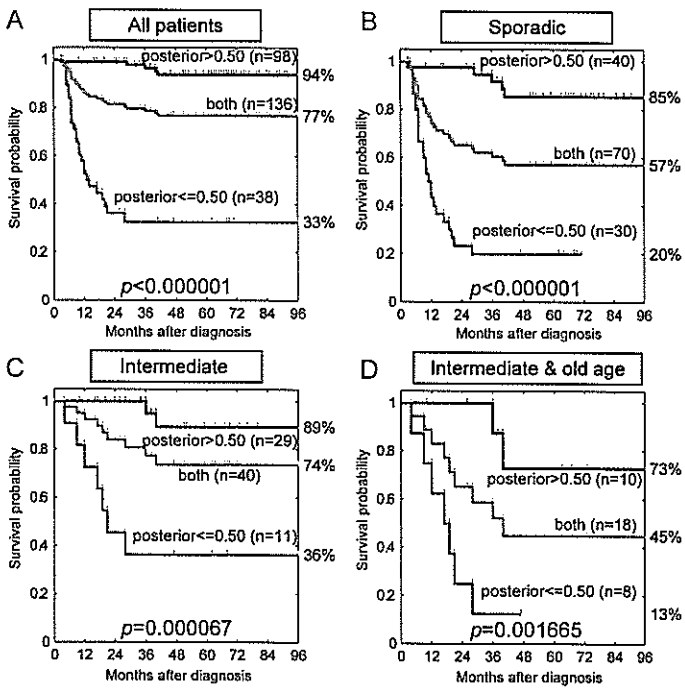

Figure 3. Disease-free survival of patients who were stratified based on the gene expression patterns

For each of the four figures, whole objective patients (green) are divided into favorable (blue) or unfavorable (red) based on the posterior values with threshold 0.5, which are calculated from gene expression patterns, and statistical features of their survival times are denoted by the Kaplan-Meier survival curves. The differences of the survival curves between the favorable (blue) and unfavorable (red) groups are evaluated by p values of the log rank test.

A and B: Survival analysis of whole and sporadic patients, respectively, divided by the supervised classifier based on microarray data.

C and D: Survival analysis of patients in the intermediate risk group with different definitions, divided by the supervised classifier. The intermediate risk group shown in (C) is defined as *MYCN* single and stage 3 or 4 (type II), and that in (D) is defined as *MYCN* single, stage 3 or 4, and older than 1 year of age.

also showed good potential to predict generally but less than the microarray, these exhibited only 64% accuracy of prediction for the type II tumors with ≥1 year of age (Table 1). Together with the results of survival analysis, the microarray classifier is revealed to be a powerful predictor to classify such group of neuroblastomas (86% accuracy; Table 1).

Practical application of 200 cDNAs microarray and independent test

For the practical use in the clinic, a cDNA microarray system that contains cDNA spots of a relatively small number and hence is easy to treat is expected. According to our gene selection based on the pairwise *F* score, the numbers of genes that were appropriate for the 5 year and 2 year prognosis prediction for all available samples were 10 and 70, respectively. In order for the system to reserve the applicability to short-term and long-term outcome prediction simultaneously, we selected 200 top-ranked genes according to the pairwise *F* scores in the 2 year prediction, because the 2 year prediction required larger variety of genes, and then made a smaller cDNA microarray system carrying the 200 genes. The newly designed microarray system (the mini-chip system) was evaluated by being hybridized with 5 μg total RNA obtained from 50 independent test samples. To preserve the independence of experimental procedure, these RNAs were prepared and hybridized in a different laboratory from the original experiments of 136 samples with the 5340 genes system (see Experimental Procedures). Although the weight values in the weighted voting classifier were determined by the 5340 genes system without any information leakage from the 50 independent samples, the result was as good as that obtained by the 5340 cDNA microarray analysis (90% [45/50] for 2 year, and 87.8% [43/50] for 5 year prognosis prediction; Figure 4B). This test validated not only the prediction robustness of our classifier constructed by the 5340 genes system, but also the construction procedure of the mini-chip system according to our gene selection based on pairwise *F* scores. When we reconstructed another supervised classifier by applying the LTO analysis to the 50 samples measured by the mini-chip system, the accuracy of the 5 year prediction was 91.8% (45/49) (Figure 4C). These results suggest